JGR Earth Surface

Key Points:

- Seafloor observations and hydrological modeling are used to investigate bedrock channels on a major Antarctic palaeo-ice stream bed
- Episodic releases from subglacial lakes modulated water availability under an expanded ice sheet driving channel incision in multiple stages
- Recharge and drainage of subglacial lakes are predicted to occur on timescales of tens to hundreds of years

Author Contributions:
Conceptualization: K. A. Hogan, R. D. Larter, J. A. Dowdeswell
Formal analysis: K. A. Hogan, N. S. Arnold, J. D. Kirkham, R. Noormets, N. R. Golledge
Funding acquisition: R. D. Larter, J. A. Dowdeswell
Investigation: K. A. Hogan, R. Noormets, C. Ó Cofaigh
Methodology: K. A. Hogan, N. S. Arnold, R. D. Larter
Project Administration: R. D. Larter, J. A. Dowdeswell
Resources: N. R. Golledge

Subglacial Water Flow Over an Antarctic Palaeo-Ice Stream Bed

K. A. Hogan[1] , N. S. Arnold[2] , R. D. Larter[1] , J. D. Kirkham[1,2] , R. Noormets[3] , C. Ó Cofaigh[4] , N. R. Golledge[5] , and J. A. Dowdeswell[2]

[1]British Antarctic Survey, Natural Environment Research Council, Cambridge, UK, [2]Scott Polar Research Institute, University of Cambridge, Cambridge, UK, [3]University Centre on Svalbard, UNIS, Longyearbyen, Norway, [4]Department of Geography, Durham University, Durham, UK, [5]Antarctic Research Centre, Victoria University of Wellington, Wellington, New Zealand

Abstract The subglacial hydrological system exerts a critical control on the dynamic behavior of the overlying ice because its configuration affects the degree of basal lubrication between the ice and the bed. Yet, this component of the glaciological system is notoriously hard to access and observe, particularly over timescales longer than the satellite era. In Antarctica, abundant evidence for past subglacial water flow over former ice-sheet beds exists around the peripheries of the ice sheet including networks of huge channels carved into bedrock (now submarine) on the Pacific margin of West Antarctica. Here, we combine detailed bathymetric investigations of a channel system in Marguerite Trough, a major palaeo-ice stream bed, with numerical hydrological modeling to explore subglacial water accumulation, routing and potential for erosion over decadal-centennial timescales. Detailed channel morphologies from remotely operated vehicle surveys indicate multiple stages of localized incision, and the occurrence of potholes, some gigantic in scale, suggests incision by turbulent water carrying a significant bedload. Further, the modeling indicates that subglacial water is available during deglaciation and was likely released in episodic drainage events, from subglacial lakes, varying in magnitude over time. Our observations support previous assertions that these huge bedrock channel systems were incised over multiple glacial cycles through episodic subglacial lake drainage events; however, here we present a viable pattern for subglacial drainage at times when the ice sheet existed over the continental shelf and was capable of continuing to erode the bedrock substrate.

Plain Language Summary Some 20,000 years ago, during the Last Glacial Maximum, Marguerite Trough on the continental shelf of West Antarctica, was occupied by a major fast-flowing ice stream. Now the seafloor of the trough is incised by a series of interlinked channels cut into the bedrock. These huge channels are similar to others found offshore Antarctica, for example, in Pine Island Bay, and were formed by pressurized water flowing underneath past ice sheets. Still, very little is known about the exact timing or mechanisms of channel formation. In this study, we present a combination of seafloor observations and numerical modeling of water flow under the ice to investigate processes of channel erosion, and whether incision occurs during all stages of a glacial cycle. Detailed seafloor morphology and imagery from a remotely operated vehicle, show that incision processes include the formation of circular potholes by swirling water, as well as the formation of smaller channels, within much larger channel tracts that were probably mostly filled with ice widening their upper parts. Interestingly, our model results suggest that water under the retreating ice stream may have been trapped in seafloor depressions, as subglacial lakes, and was then released periodically every few tens to hundreds of years.

1. Introduction

1.1. Background and Context

Deglaciated terrains contain abundant evidence for past subglacial water flow (e.g., Bjarnadóttir et al., 2017; Lowe & Anderson, 2003; Shaw & Gilbert, 1990; Sugden et al., 1991) and have the potential to provide important information about the form and connectivity of subglacial hydrological systems, as well as the geological composition of the beds they traverse. Such terrains can be studied at all spatial scales and are relatively easy to access when compared with contemporary subglacial settings. Additionally, in marine environments these terrains are often almost completely untouched by destructive post-glacial processes, either natural or anthropogenic in nature. As such, deglaciated terrains represent useful complementary datasets to modern borehole

Supervision: R. D. Larter, J. A. Dowdeswell
Visualization: K. A. Hogan, R. Noormets
Writing – original draft: K. A. Hogan, N. S. Arnold
Writing – review & editing: R. D. Larter, J. D. Kirkham, C. Ó Cofaigh, J. A. Dowdeswell

or over-ice geophysical observations and numerical modeling experiments targeting subglacial water flow and associated bed properties.

Around Antarctica, erosive landforms (channels, corrugated surfaces, basins and cavities, potholes) produced by past subglacial water flow occur under the extant ice sheet (e.g., Jamieson et al., 2016; Jordan et al., 2010; Rose et al., 2014), and in areas beyond the ice margin including ice-free terrestrial areas (e.g., Denton & Sugden, 2005; Lewis et al., 2006; Sawagaki & Hirakawa, 1997; Sugden et al., 1991), and marine areas on the inner continental shelf (e.g., Anderson & Oakes Fretwell, 2008; Domack et al., 2006; Graham et al., 2010; Lowe & Anderson, 2003; Nitsche et al., 2013; Simkins et al., 2017; Kirkham et al., 2019, 2020). In the latter setting, the largest and most widespread features are huge networks of channels incised into bedrock and found mostly within cross-shelf troughs carved by palaeo-ice streams during previous glacial periods. The undulatory long profiles of the channels, containing both positive and negative slope gradients, their anastomosing patterns, and their abrupt terminations are taken as clear evidence that they formed subglacially (Benn & Evans, 2010; Shreve, 1972). The bedrock channels often link larger elongated basins which are sometimes interpreted as the locations of former subglacial lakes both from their morphology and their sedimentary infill sequences (e.g., Domack et al., 2006; Kirkham et al., 2019, 2020; Kuhn et al., 2017). Thus, these channels are typically interpreted as having been incised by pressurized subglacial water moving between storage locations in subglacial lakes (Domack et al., 2006; Kirkham et al., 2019, 2020; Nitsche et al., 2013). Hydrological modeling over one such channelized area in Pine Island Bay has confirmed that the water produced by basal melt in Antarctica would not have been sufficient to maintain continuous flow in the channels, or to erode them (Kirkham et al., 2019), and ideas are now converging on channel formation by episodic discharges sourced from upstream subglacial lakes (Kirkham et al., 2019, 2020; Nitsche et al., 2013). However, questions remain regarding the exact timing of both initial channel incision (cf. Kirkham et al., 2020), and during which stage (or stages) of a glacial cycle the massive discharges required to incise bedrock are released. Some authors have considered the trapping and release of sea water in topographic basins during ice-sheet advance as the source of the flood waters (Alley et al., 2006), whereas an alternative model suggests that water trapped during advance is only released during the retreat phase (Jordan et al., 2010). In either case, the filling and episodic release of water from Quaternary Antarctic subglacial lakes at ice-sheet catchment scales is a different process to that considered for many landforms incised by subglacial water in the Northern Hemisphere. There, Nye channels, tunnel valleys, eskers, hummocks and so-called "meltwater corridors," spatially extensive assemblages of meltwater-related landforms, form later in the glacial-deglacial cycle as the climate ameliorated and more surface meltwater was potentially available at the ice-bed interface via surface-to-bed connections (e.g., Kehew et al., 2012; Lewington et al., 2020; Peterson & Johnson, 2018; Storrar et al., 2014). We do note, however, that there are examples of relict meltwater features from deglaciated terrains in both hemispheres that cut across topographic lows, but at high elevations, indicating their association with "full glacial" conditions (e.g., Denton & Sugden, 2005; Glasser & Sambrook Smith, 1999; Sugden et al., 1991). Thus, the picture is more complex than one process for Antarctic glacial channel formation and another for Northern Hemisphere channels.

Regardless of the timing of subglacial water release, strong feedback effects between the subglacial hydrology and dynamics of the overlying ice mean that there was almost certainly a response in the ice sheet. This is because basal water can either facilitate basal sliding thereby promoting fast ice flow, or, if the hydrological system is channelized, it can drain the bed efficiently leading to more "sticky" basal conditions (through increased basal traction) and retard flow (e.g., Bell, 2008; Kamb et al., 1985). In the scenario of subglacial water release during glacial advance, previous work has hypothesized that this could promote or initiate ice streaming in a juvenile ice sheet causing a significant shift in the dynamics of the ice sheet (Alley et al., 2006; Bell et al., 2007). For the extant ice sheet, remote-sensing observations at Byrd Glacier in East Antarctica confirm that episodic subglacial lake drainage events have caused short-term (several months) accelerations in the velocity of the overlying ice (Stearns et al., 2008), although several other studies show no discernible increase in downstream flow velocities following lake drainage events (Joughin et al., 2016; Smith, Gourmelen, et al., 2017). During deglaciation when the ice sheet is already decaying, it has been suggested that a release of subglacial water may cause further destabilization via decoupling from the bed or enhanced ice streaming. Therefore, many questions remain about the duration of any ice-dynamical response to such changes in subglacial hydrological conditions, as well as their significance within phases of widespread retreat.
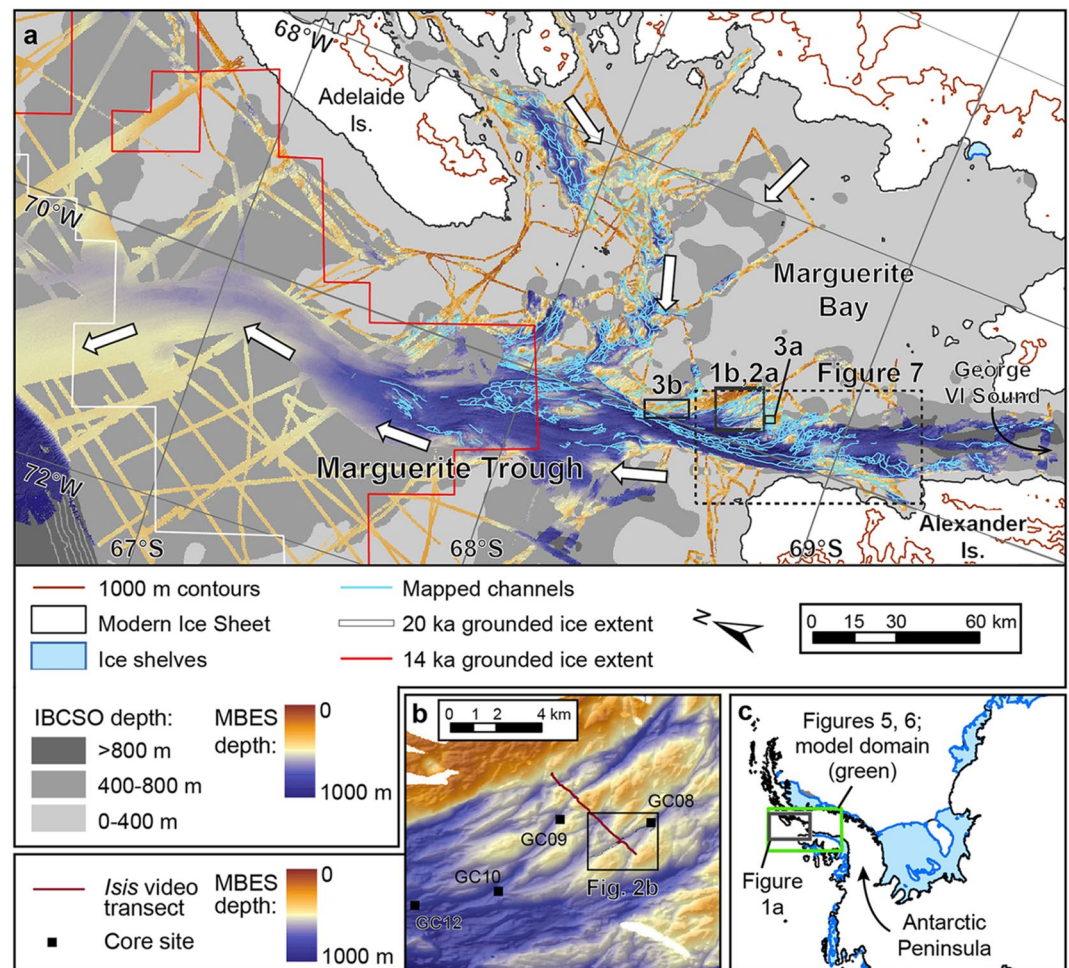
Figure 1. Marguerite Trough palaeo-ice stream bed and data locations. (a) Compilation of multibeam echosounder (bathymetry) data in Marguerite Trough, a major palaeo-ice stream bed. Mapped channels (blue lines) and ice-stream flow directions (white arrows) are also shown; regional bathymetry is from IBCSO (Arndt et al., 2013). (b) Inner shelf anastomosing channel network with locations of sediment cores and remotely operated vehicle (ROV) dives (located in a). (c) Map of the Antarctic Peninsula and Weddell Sea sector of Antarctica showing the location of the study area in (a) and later figures.

Here, we focus on the scenario of meltwater release during the Last Glacial Maximum (LGM) and during a phase of glacial retreat using a combination of detailed geoscientific observations and numerical modeling for a large channel system on a well-surveyed palaeo-ice stream bed in Marguerite Trough, West Antarctica. We use ship-board bathymetry, sediment cores and remotely operated vehicle (ROV) dive data in the form of high-resolution bathymetry and seafloor imagery, to investigate channel incision processes. Then, using a hydrological model, driven by ice-sheet model outputs, we quantify the rates of subglacial lake fill and drainage for the LGM (c. 20 ka) and during deglaciation when the channels were still covered by ice (14 ka). By scaling the model outputs to modern observations of subglacial lake drainages we predict the magnitude and frequency of episodic drainage events through the Marguerite Trough palaeo-ice stream catchment.

1.2. Marguerite Trough Palaeo-Ice Stream Bed

Marguerite Trough, located just offshore of the southern end of the western Antarctic Peninsula (Figure 1), is a 370-km-long sinuous cross-shelf trough that was occupied by a fast-flowing palaeo-ice stream during the last glacial (Livingstone et al., 2013; Livingstone, Cofaigh, et al., 2016; Livingstone, Stokes, et al., 2016; Ó Cofaigh et al., 2002, 2005). At that time, it drained an area of c. 60,000 km^2 and had an estimated ice flux of 20 km^3 yr^{-1}

at the 80-km-wide shelf-edge grounding line (Dowdeswell et al., 2004). Reconstructed and modeled ice-flow directions (Ó Cofaigh et al., 2002, 2005; Livingstone et al., 2013; Golledge et al., 2013) confirm that Marguerite Trough was a major ice-drainage pathway for the Antarctic Peninsula Ice Sheet during the last glacial period (cf. Ó Cofaigh et al., 2014).

The inner part of the trough has a rugged morphology identified as crystalline bedrock on seismic reflection profiles, mantled by a generally thin drape of till and Holocene sediment (Kennedy & Anderson, 1989). The evidence for subglacial water flow in Marguerite Trough includes the widespread occurrence of anastomosing to dendritic channels with undulatory profiles on the inner and middle continental shelf (Figure 1a, Anderson & Oakes Fretwell, 2008; Hogan et al., 2016; Kirkham et al., 2020; Ó Cofaigh et al., 2002, 2005). The channels are up to 2,900 m wide and 200 m deep (mean values are 400 and 40 m, respectively; Kirkham et al., 2020), and suggest water routing into and along the trough; that is, approximately parallel to palaeo-ice flow directions (Figure 1a). East of the inner trough, in Marguerite Bay, are a series of basins and channels up to 300 m deeper than the surrounding bedrock (Anderson & Oakes Fretwell, 2008; Livingstone et al., 2013).

The deglaciation history of Marguerite Trough is reasonably well known from studies of submarine glacial land-forms and ^{14}C dating of overlying associated marine sediments (Anderson & Oakes Fretwell, 2008; Heroy & Anderson, 2007; Kilfeather et al., 2011; Livingstone et al., 2013; Livingstone, Cofaigh, et al., 2016; Livingstone, Stokes, et al., 2016; Ó Cofaigh et al., 2002, 2005). These studies show that rapid retreat from the shelf edge had begun before 14 ka before slowing and retreating across the mid-shelf in a step-wise pattern. The rate of ice retreat then accelerated again to leave the ice margin located on the inner shelf by c. 10–9 ka (Bentley et al., 2011; Kilfeather et al., 2011; Prothro, 2018). The widespread deposition of well-sorted silts in the bedrock basins of Marguerite Bay at that time may be related to the release of glacial meltwater from 13–10 ka (Prothro, 2018). However, the origin and timing of any meltwater release, which may have been very gradual - is unknown, as is what, if any, effect this had on the dynamics of the ice sheet in the area. By acquiring geological evidence from this palaeo-ice stream terrain and integrating it with numerical modeling we aim to provide new information on subglacial hydrological conditions during glaciation of the trough, and how this striking terrain with numerous, large, interconnected bedrock channels developed.

2. Materials and Methods

2.1. Marine Datasets

Channel morphology and sediment infill in Marguerite Trough was investigated using three sets of marine observations. First, bathymetric information was from shipborne multibeam echosounder (MBES) datasets, providing medium resolution (20–40 m cells) gridded bathymetric data for much of Marguerite Trough, including the channel systems (Figures 1a and 1b). Data were acquired during eight cruises of the polar research vessels RRS *James Clark Ross* (JR) and RVIB *Nathaniel B. Palmer* (NBP) (JR: 59, 71, 157-166, 165; NBP: 0103, 0104, 0201, 0202) using either a Kongsberg EM120 or a Seabeam 2112 (all NBP cruises) deep-water MBES. Bathymetric soundings were processed in Kongsberg Neptune or MB-System softwares shortly after acquisition by removing erroneous points and correcting for sound velocity variations. Processed soundings were downloaded from the the relevant US and UK data centers (see Data Availability statement) and gridded in MB-System. Vertical precision of the two systems was 0.5% of the water depth. Subsurface sediment layers in the channels were also investigated during cruises JR59, JR71 and JR157 using a shipboard TOPAS PS018 sub-bottom profiler echo-sounder. However, data quality was severely hampered by side echoes from steep channel walls and compounded by the relative narrowness of the channels compared with typical vessel survey speeds (8–10 knots). This was the case even during ROV dives when vessel speeds were considerably slower.

Second, during cruise JR157 the *Isis* ROV completed two dives in a channel system on the inner shelf (Figures 1b and 2b). For one of the dives, the ROV was flown at a constant altitude of ~20 m above the seafloor and was equipped with a Kongsberg Mesotech SM2000 MBES configured to survey the seafloor in detail (0.5 m grid-cell size, vertical resolution ~0.01 m). For the second dive the ROV was configured for a video survey but seafloor depths were also recorded by a single-beam echosounder; bottom photographs were acquired on both dives. Navigation data for shipboard instruments were acquired using differential GPS. The *Isis* ROV made use of a shipboard ultra-short baseline acoustic navigation system to obtain frequent absolute position fixes (each with RMS error of about 5 m; Dowdeswell et al., 2007) alongside an onboard fibre-optic gyrocompass.
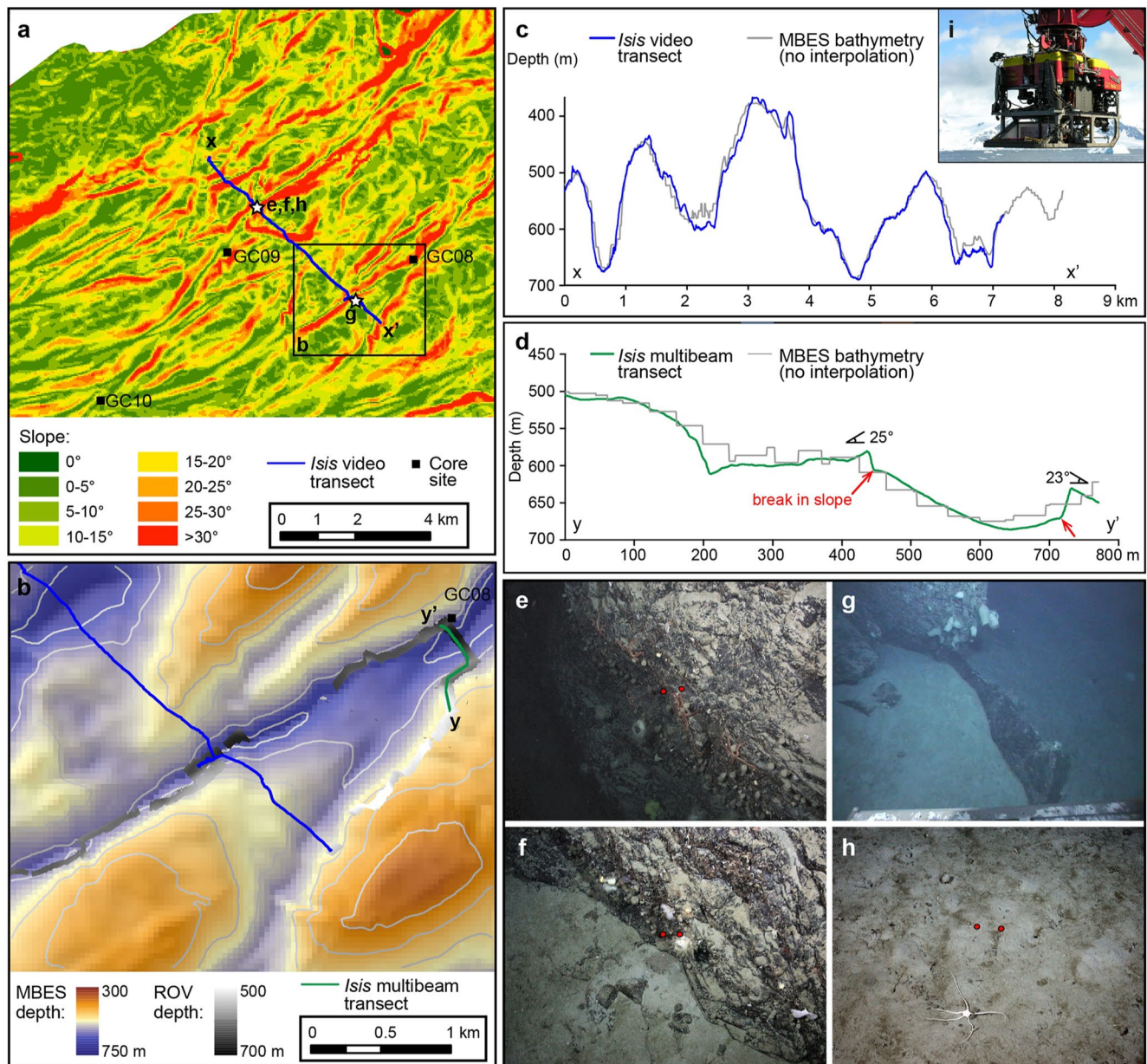
Figure 2. Detailed marine observations of the inner shelf channel system. (a) First derivative of bathymetry, slope, over the channels (same area as Figure 1b). (b) Location of remotely operated vehicle (ROV) video survey line and multibeam surveys near the GC08 core site (located in Figures 1b and 2a). (c and d) Comparison of seafloor profiles from shipborne MBES and ROV bathymetry over bedrock channels (located in 2a, 2b). (e–h) ROV bottom photographs (e, f, h) and video stills (g) showing the character of the seafloor in the bedrock channel system. The red circles in (e, f, h) are 10 cm apart; the frame in (g) is about 1 m wide (photos are located in 2a). (i) *Isis* ROV being deployed during JR157.

The third marine data set consists of seafloor sediment samples from four geological cores up to 3.34 m in length. These were also collected during JR157 using a gravity corer in the same channels explored by the *Isis* ROV (Figure 1b; Table 1). Core sites targeted the downstream confluences of several anastomosing channels where sediments deposited from subglacial meltwater might accumulate. Physical properties (magnetic susceptibility, gamma density, *p*-wave velocity, and fractional porosity) were measured (or calculated from measurements, i.e., porosity) on the whole cores using a GEOTEK multisensor core logger. The cores were described with respect to particle size, sedimentary structures, bed contacts, sorting, geometry, clast shape and texture. Shear strength measurements (to help differentiate between diamictons produced in subglacial or proglacial settings; cf. Ó Cofaigh et al., 2005) were performed at 10-cm intervals using a hand-held shear vane. Grain size and

Table 1
Location, Water Depths and Recovery of Marine Sediment Cores

Core	Latitude (S)	Longitude (W)	Water depth (m)	Core length (m)
GC08	68° 42.4038′	69° 38.2438′	623	2.09
GC09	68° 39.8985′	69° 40.4904′	675	3.00
GC10	68° 38.94.86′	69° 47.5910′	767	3.34
GC12	68° 36.8237′	69° 50.9231′	801	2.64

water content analyses were also performed on sediment samples taken every 10 cm down-core. The samples were weighed, disaggregated in deionised H_2O and passed through a 2-mm and a 63-μm sieve and each of the size fractions (mud <63 μm, sand 63 μm–2 mm, gravel >2 mm) was collected, dried and weighed. The proportions of mud, sand and gravel were determined on the basis of weight, and water content was determined by subtracting the total dry weight from the wet weight.

2.2. Subglacial Hydrological Modeling

To calculate subglacial water flow paths and fluxes in the Marguerite Trough channel systems, we used the results of the ice-sheet model experiments of Golledge et al. (2014) for two time periods during the last glaciation, 20 ka (equivalent to the LGM), and 14 ka (during deglaciation). In our analysis, we focus on the deglacial stage following the LGM because ice-sheet reconstructions and numerical models are much better constrained during retreat than for advance phases; this is evidenced by the common approach to "spin-up" numerical models to match the LGM ice-sheet geometry (thickness and extent) and then run simulations of the deglaciation to match geological and ice-core evidence for specific time periods (e.g., Golledge et al., 2012, 2014). We posit that the hydrological modeling results we present may be comparable for an ice sheet advancing in to Marguerite Trough with a similar configuration to the 14 ka simulation; however, this is difficult to test without robust model simulations for the advance phase. Such an advancing ice sheet may have had a shallower surface slope, due to slow cooling and ice-sheet growth (vs. rapid warming and retreat), and therefore have been more susceptible to dynamic changes related to any subglacial water releases at that time (cf. Larter et al., 2019). Then again, we might also expect more second-order dynamic variability during retreat as ice streams thickened, accelerated and thinned in response to oceanic warming. Thus, we maintain that the hydrological modeling simulations for 14 ka are likely to be at least representative for an advancing Antarctic ice sheet, as well as the retreating one.

Subglacial hydraulic potential determines the water flow paths (Shreve, 1972) and was calculated using the modeled ice thickness and bedrock topography. The model experiments of Golledge et al. (2014) have a 15-km spatial resolution. The regional bathymetry data set, IBCSO (Arndt et al., 2013), which was adjusted for isostatic deflection to produce the bed elevation for the hydrological modeling, has a grid-cell size of 500 m. For this study, we chose to run the hydrological modeling at 500-m resolution because the large bedrock channels in Marguerite Trough are, in general, spaced more than 500 m apart meaning that major channels were resolved by the model whilst run times remained relatively low. To convert the kilometer-scale ice-sheet model results to the 500-m bathymetry data resolution, we first calculated the modeled isostatic deflection for the two time periods, interpolated the deflection to 500 m-resolution, and added this to the present-day bed elevation data (Figure S1a). We also interpolated the modeled ice-sheet surface elevation to 500 m-grid spacing (Figures S1b and S1c) and then subtracted the isostatically corrected 500-m bed topography to produce a 500-m grid of ice thickness for each time period.

Subglacial hydraulic potential (ϕ) was then calculated from the bedrock topography and ice thickness:

$$\phi = \rho_w g h + k \rho_i g Z \tag{1}$$

where ρ_w and ρ_i are water and ice density respectively, g is gravity, Z is the ice thickness, h is the bed elevation and k is a parameter which can be varied between 0 and 1 in order to simulate the effect of variable subglacial water pressure (Shreve, 1972). Higher k values represent higher water pressure, with $k = 1$ indicating that the subglacial water pressure is equal to the ice overburden pressure, and $k = 0$ for zero subglacial water pressure. Water pressure beneath ice sheets is typically close to the ice overburden pressure (e.g., Flowers, 2015); given that we do not model basal hydrology in detail, we used k values of 0.8, 0.9, and 1.0 in our calculations to simulate a range of possible basal water pressures.

In order to calculate the possible subglacial water fluxes, we also needed to quantify subglacial meltwater production over the trough. This was calculated using the modeled basal friction and geothermal heat flux for areas where the ice-sheet model indicates basal water is present and the bed is at the pressure melting point (for full details of the method see Kirkham et al., 2019). For areas with temperatures below the pressure melting point,

Table 2
Lake Volume (V, km³), Steady-State Discharge (Q, m³ s⁻¹) and Turnover Time (T, Years) for the Lakes Along the Main Drainage Axis Shown in Figure 5

a. 20 ka	k = 0.8			k = 0.9			k = 1.0		
Lake	V	Q	T	V	Q	T	V	Q	T
A	41.3	6.7	194.3	11.7	6.6	56.3	0.4	5.4	2.6
B	2.3	6.2	11.9	1.7	6.0	8.7	1.1	4.9	6.8
C	1.7	5.9	9.2	0.6	5.8	3.5	*0.02*	*4.7*	*0.1*
D	1.0	5.1	6.5	0.5	5.0	3.4	*0.05*	*4.0*	*0.4*
E	4.7	4.4	33.5	1.5	4.3	11.1	*0.02*	*3.5*	*0.2*
F	5.4	0.9	195.9	2.6	2.1	38.9	1.56	0.2	214.9
G	32.5	0.4	2615	11.3	0.4	899.8	0.4*	0.4*	31.4*
H	14.8	1.2	384.1	5.7	0.8	228.1	0.3	0.5	19.2
b. 14 ka	k = 0.8			k = 0.9			k = 1.0		
Lake	V	Q	T	V	Q	T	V	Q	T
A	49.6	9.6	163.5	21.1	9.9	67.8	1.6	10.3	4.9
B	2.1	8.1	8.1	1.7	7.7	6.9	0.3	7.8	1.2
C	2.1	7.6	8.8	0.9	7.3	4.1	*0.1*	*7.5*	*0.6*
D	1.2	6.7	5.7	0.6	6.4	3.2	*0.2*	*6.6*	*0.8*
E	10.1	5.9	54.1	6.2	5.6	35.3	3.3	6.0	17.6
F	0.9	0.8	38.4	*0.2*	*0.8*	*9.0*	-	-	-
G	21.2	0.6	1267	7.4*	0.5*	434.3*	1.2*	0.5*	81.7*
H	10.7	1.3	259.2	3.7	0.7	166.5	*0.2*	*1.0*	*4.9*

Note. a. =20 ka; b. =14 ka. Italics denote lakes with a volume of less than 0.25 km³, which are not shown in Figures 5, 6 or 7. * Denotes where one large lake splits into two adjacent lakes at different *k* values. – denotes no lake at location.

the basal melt was set to 0. These values were also interpolated to 500-m spacing. To assess the propagation of uncertainty from the ice-sheet model simulations to the hydrological modeling we have to consider the uncertainty of the ice-sheet model runs. Golledge et al. (2014) present this in the form of the mismatch between the modeled ice thickness output (at the end of the ice-sheet model runs) and the present-day Antarctic Ice Sheet, which is on average about 11%. We note that varying the value of *k*, as we have done here, is actually analogous to changing the ice thickness for the hydrological potential surfaces and routing. For example, 100% ice thickness with *k* = 0.9 is the equivalent of 90% ice thickness with *k* = 1.0. Thus, we can say that the uncertainty in the ice-sheet model runs would produce hydrological modeling results across the same range as we have presented for varying *k* values (see Table 2).

The steady-state basal water flux was calculated using an upstream area algorithm developed by Arnold (2010), with each digital elevation model (DEM) cell assigned a weight equal to the volume of subglacial meltwater production per unit time. Unlike most upstream area algorithms, which require depressions in the bed surface to be filled from water upstream, this algorithm allows closed basins in the DEM surface to fill with water, and overspill downstream at the calculated position of the depression outlet, preserving the connectivity within the system. Each closed basin within the DEM has a defined catchment (the set of higher DEM cells which flow into that basin); the algorithm also identifies the lowest DEM cell on the catchment boundary, which forms the outlet from the catchment. The algorithm identifies all the "flooded" cells (those lower than the outlet cell) within a catchment, which allows lakes to be identified, and their areas, depths (from the outlet elevation and the individual cell elevations) and volumes to be calculated.

The weighted upstream area calculation effectively gives the steady-state water flux in each DEM cell. Cells within a lake are assigned the flux calculated for the lowest cell within each catchment. This value is then used as the weight in the outlet cell (plus any local basal melt), and is passed downstream into the next catchment until ultimately the edge of the model domain is reached. Using the flux calculation for each lake, and the lake volume, the time taken for each lake to fill (assuming steady water flow, and that all lakes are full so water

flows downstream continuously) can be calculated. If lake drainage is assumed to occur once a lake has filled, this effectively gives us the "turnover time" for each lake (Kirkham et al., 2019; Willis et al., 2016; Wingham et al., 2006), assuming that the lake drains fully every time that it drains.

3. Evidence for Past Water Flow in Marguerite Trough

3.1. Observations From Marine Datasets

The ROV data, combined with shipborne bathymetry, provide detailed morphological information for the inner shelf anastomosing channels (Figure 2) not captured in regional morphometric analyses. Maps of the first derivative of bathymetry, slope, show that the largest channels have steep sides of 20°–40°, but reach 60° locally, and low-gradient floors (<10°) (Figure 2a). This is supported by ROV bottom photographs of what appear to be near vertical channel walls extending all the way to the channel floor, complete with attached fauna (for example, the sponges are *Rosella* species including *R. nuda*, *R. racovitzae*, and *R. villosa*) extending out horizontally (Figures 2e and 2f). Video footage from the ROV video transect moving up one of the channel sidewalls confirms the steep nature of the channel sides (see Movie S2) and even suggests possible undercutting at the base of some channels. We note that MBES mapping systems set up for seafloor mapping (i.e., vertical look direction) cannot record two values for depth (z) at any one location (x, y) as one of them will always be in the shadow of the other, meaning that it is not possible to map any potential undercutting in this way. A horizontal (forward or side) look direction, as has been set up for habitat mapping in canyons (Huvenne et al., 2011) and to map the faces of tidewater glaciers (Rignot et al., 2015), would be needed to fully map the form of the channel walls.

Cross-sectional geometries for the channels vary between v- and u-shaped (e.g., Figure 2c) although v-shaped forms are more prevalent; this is consistent with regional morphometric analyses of the channels (Kirkham et al., 2020). However, when the channel floors are wide and flat (i.e., trapezoidal or u-shaped cross-sections) the ROV bathymetry shows that they can have complex morphologies including overdeepenings along the sidewalls, floors that are rugged on scales of tens of meters (up to a few hundred meters), and stepped sidewall profiles. For example, a cross-section through the high-resolution ROV bathymetry data (Figures 2c and 2d) appears to show that the sidewall steps are very steep (60°–80° slopes), tens of meters high (20–80 m), and their surfaces can also be rugged. The more horizontal limbs of the steps at the base of the channel appear to dip toward the outside of the channel with slopes of 20°–25° potentially indicating overdeepening along the outside edges of the channel on the surface of individual steps, although we acknowledge the small areal data coverage of the ROV bathymetry. Close inspection of a 1500-m wide confluence area on the south-western side of the channel system reveals a series of small interlinked channels crossing the confluence floor (Figure 3a). The channels are several hundreds of meters wide, tens of meters deep, and often have v-shaped cross-sectional geometries.

In addition to possible undercutting of the channel sidewalls, ROV bottom photographs and video footage from the base of the sidewalls shows several phenomena. First, the sediment infilling the channel often forms a ramp, which from bottom photographs appears to be a few meters high and sloping away from the sidewall to the channel floor (Figure 2f). This indicates that cross-sectional geometries are certainly modified by sediment infill at least on meter-scales. The channel cross-section in Figure 2d, extracted from the ROV bathymetry, appears to show evidence of similar infill but at a larger scale between the two deepest "steps" in the channel sides. There, clear breaks in slope (arrowed) differentiate the steps from the broad v-shape of the channel base with slopes of 15°–25°. Second, small potholes (estimated diameter of several meters) were occasionally visible on the channel floor at the base of channel sidewalls, although they were partially infilled with marine sediments (Figure 2g). A much larger circular depression that we also interpret as a pothole (diameter 1,200 m; depth 200 m) occurs on the shoulder of Marguerite Trough just north of the channel system in a present-day water depth of ~200 m (Figure 3b). Several other isolated depressions with flat bottoms that may also be potholes (diameters 500–700 m, depths 100–120 m) occur on the trough shoulder about 10 km further north in water depths of 300–600 m (Figure 3c). We note the similarity in diameter-scale of these potholes to glacitectonic hill-hole pairs in Anvers Trough (Larter et al., 2019), which form when sedimentary material is frozen to the base of the ice sheet and transported forwards *en masse*. However, we suggest the relatively smooth circular shape of the largest pothole, the significant depth of the (hard rock) features compared with the (sedimentary) hill-hole pairs (depths ~20 m), and their proximity to the huge channels are evidence for a process beyond simple glacial plucking and involving erosion by subglacial water.
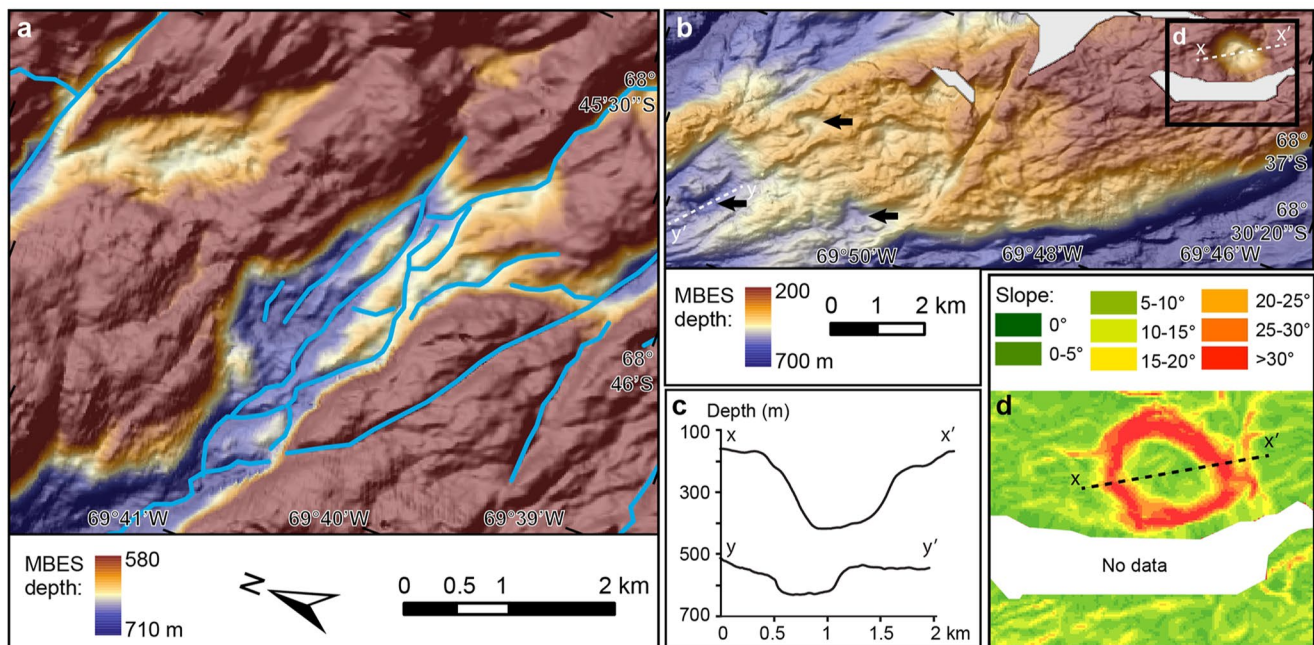
Figure 3. Geomorphic features of interest in or near the inner shelf channel system. (a) Network of small channels in a confluence area. (b) Giant potholes identified on the flank of the Marguerite Trough (located in Figure 1a). (c) Seafloor profiles through the potholes in (b). (d) Slope map of the largest pothole.

Sediment core samples were the primary data set used to investigate channel infill. Of the four sediment cores recovered from the inner shelf channel system, GC08 and GC09 were acquired in channels and cores GC10 and GC12 targeted outwash material from relatively flat seafloor areas beyond channel mouths (Figure 1b). The upper units in all cores (203–293 cm thick) were homogeneous bioturbated olive-gray muds with various amounts of sand-, gravel- and pebble-sized grains dispersed throughout (Figure 4). This is a common lithofacies for Holocene post-glacial deposits in Marguerite Trough (Kennedy & Anderson, 1989; Kilfeather et al., 2011; Ó Cofaigh et al., 2005). Below the upper unit was either a massive, dark gray diamicton (GC10, GC12), or thin sandy to pebbly mud units (GC08, GC09). The diamictons are matrix-supported, muddy to sandy diamictons with dispersed subangular and agglutinated pebble-sized clasts. Shear strengths are up to 20 kPa. In Marguerite Trough, diamictons with massive structure and low shear strengths (<40 kPa) have been interpreted as dilatant subglacial tills formed by a combination of deformation and localized lodgement (cf. Kilfeather et al., 2011; Ó Cofaigh et al., 2005, 2007). The other facies underlying the upper muds, pebbly muds, sands, and intercalated muds/diamictons (Figure 4), are interpreted as evidence of the transition from a subglacial to proximal glacimarine to distal glacimarine/seasonally open marine environment but with the area covered by an ice shelf during the transition from subglacial to ice proximal (Domack et al., 1999; Smith, Andersen, et al., 2017; Smith et al., 2019). No sorted sediments were recovered in the cores from the channels or downstream areas; this is consistent with previous studies from such channel settings (cf. Smith, Hillenbrand, et al., 2009).

3.2. Modeled Subglacial Water Flow

Calculated steady-state basal water fluxes for the inner Marguerite Trough subglacial catchment, which continues as a large linear overdeepening into George VI Sound (Figure 1a), are presented in Figures 5 and 6 for 20 and 14 ka, respectively. Water fluxes are shown for a range of k values (0.8, 0.9, and 1.0), as are the calculated volumes and turnover times for each predicted lake. Given the large number of small depressions in the hydraulic potential surfaces, particularly for lower k values, we only show lakes with calculated volumes greater than 0.25 km³, the mean value for Antarctic subglacial lake drainage events reported by Smith, Fricker, et al. (2009). In all cases, there is a clear linear drainage pattern along the axis of George VI Sound and Marguerite Trough. The catchment area feeding the trough increases slowly in width upstream before bulging to the east (toward the Antarctic Peninsula), as a series of tributary drainage axes enter the main axis from that direction. Although this broad pattern is repeated for the three k values at the two time periods (Figures 5 and 6), details of the catchment
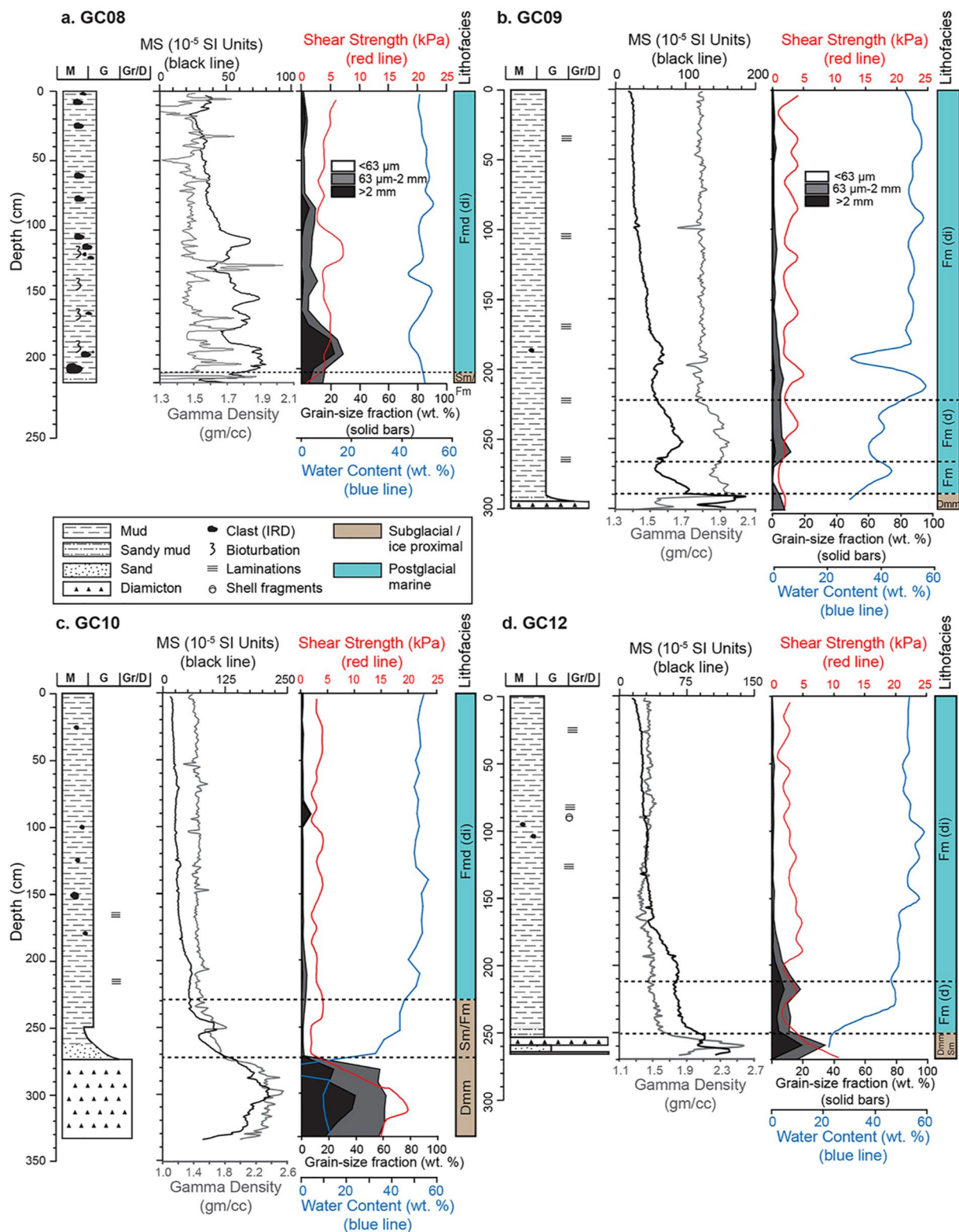
Figure 4. Sediment core logs and measured physical parameters for cores from the inner shelf channel system (located in Figure 1b). (a) GC08. (b) GC09. (c) GC10. (d) GC12.
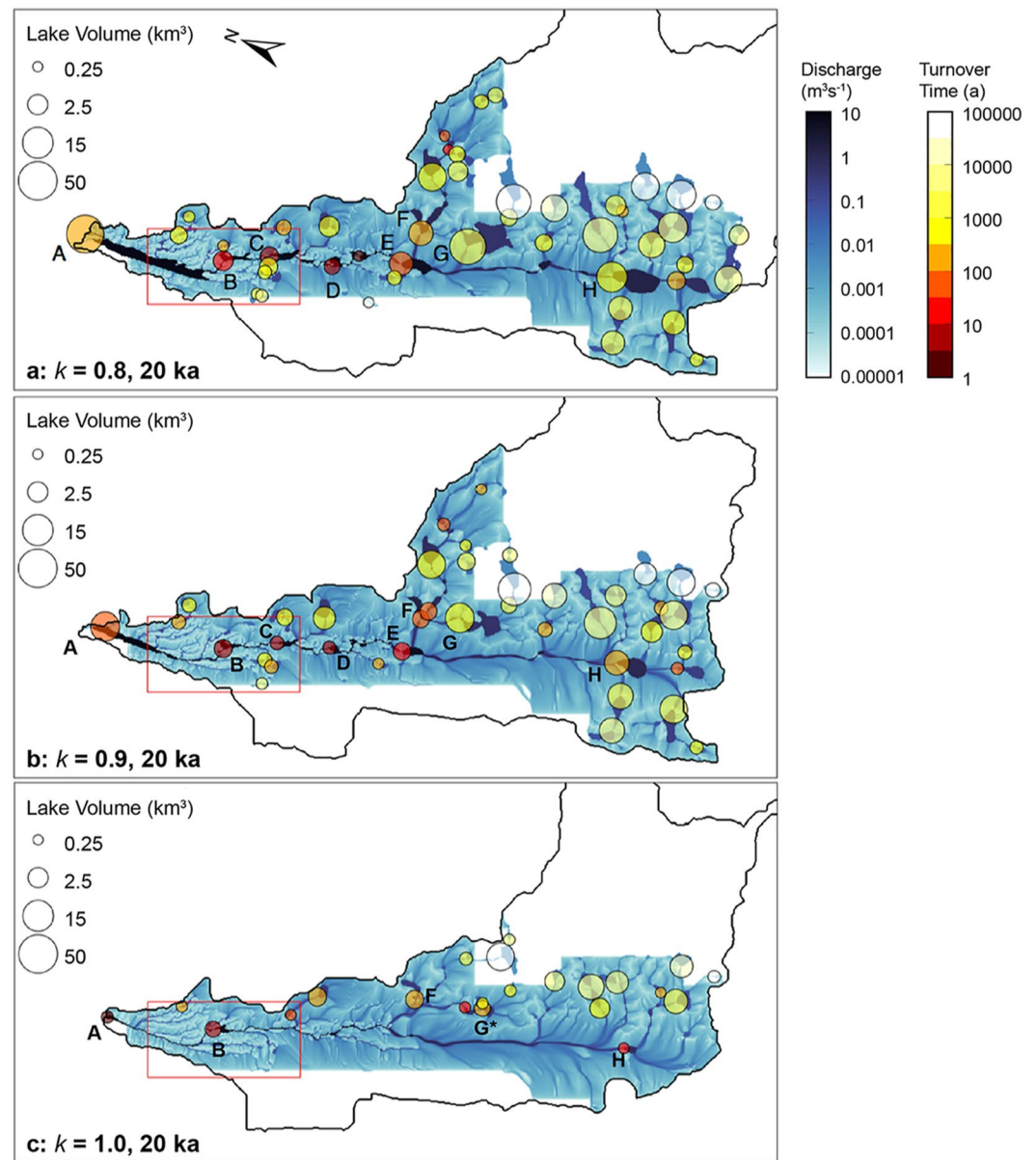
Figure 5. Calculated steady state subglacial water fluxes for 20 ka BP for (a) $k = 0.8$; (b) $k = 0.9$; and (c) $k = 1.0$. Letters show the lakes discussed in the text, and with statistics given in Table 2. Lake outlets shown as circles scaled with the log of volume, and colored by turnover time (see text). The location of the box for (a)–(c) is shown in Figure 1. Note that lake G splits into two lakes at $k = 1.0$ so is marked with a (*) as in Table 2. Black line is the modeled subglacial water catchment area for the Marguerite palaeo-ice stream bed for each model run, that is, catchments decrease in size at higher subglacial water pressures and, therefore, at higher k values. Red box is the area shown in Figure 7.

area vary with the k value, as well as for the two time periods, due to the differing subglacial potential surface in each case. Inferred lakes along the main drainage axes can also clearly be seen as "beads," particularly at lower k values.

Close examination of the area around the anastomosing channels in Figure 1b (red box in Figures 5 and 6) indicates that the route of the main drainage axis is sensitive to the k value. For 20 ka and 14 ka, and for $k = 0.8$ and 0.9 (Figures 5a, 5b, 6a, and 6b), the main drainage axis (dark blue line) exits lake B toward the west, before kinking north to form the main drainage axis along Marguerite Trough toward lake A (e.g., Figure 7a, 14 ka, $k = 0.8$ shown). At both time periods for $k = 1$, however, subglacial drainage exits lake B to the north before turning west and then north in Marguerite Trough (e.g., Figure 7b, 14 ka, $k = 1$ shown), which does not hold a large lake for
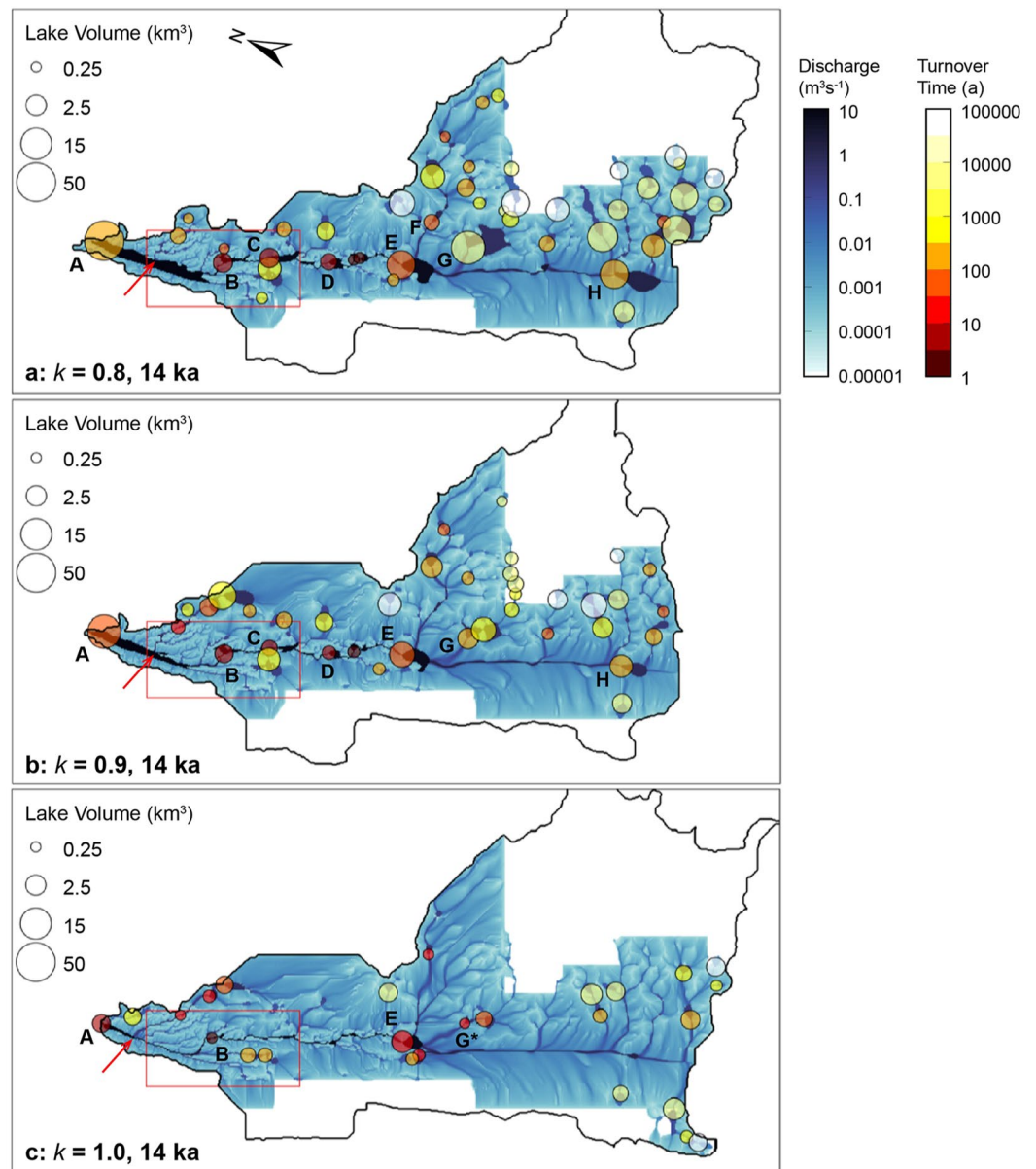
Figure 6. Calculated steady state subglacial water fluxes for 14 ka BP for (a) $k = 0.8$; (b) $k = 0.9$; and (c) $k = 1.0$. Lake outlets shown as circles scaled with the log of volume, and colored by turnover time (see text). The location of the box for (a–c) is shown in Figure 1. Note that lake G splits into two lakes at $k = 1.0$ so is marked with a (*) as in Table 2.

$k = 1$. Further north along Marguerite Trough there is another short drainage axis which enters lake A from the east at $k = 0.8$ and 0.9 but which flows north at $k = 1$, before joining the main axis closer to the catchment outlet (see red arrows on Figures 6 and 7). There are also complex changes in the area south of lakes B and C between the different k values and time periods.

Calculated lake volumes, steady state water fluxes and turnover times for the 8 lakes labeled as A to H in Figures 5 and 6 (six along the main axis, plus two large tributary lakes) are shown in Table 2 and Figure S4 in Supporting Information S1. Using k values of 0.8 or 0.9, predicted lake volumes range from <1 km³ to several tens of cubic kilometres but the volumes decrease drastically as the k value increases, that is, with increasing higher subglacial water pressures. For example, all of the lakes we report except for two (B, F) lose 95%–99% of their volume when going from assuming $k = 0.8$ to $k = 1.0$ (Figures S4a and S4b in Supporting Information S1); the same six lakes lose 50%–72% of their volumes between $k = 0.8$ and $k = 0.9$. Lake discharges are generally low (<10 m³ s⁻¹)
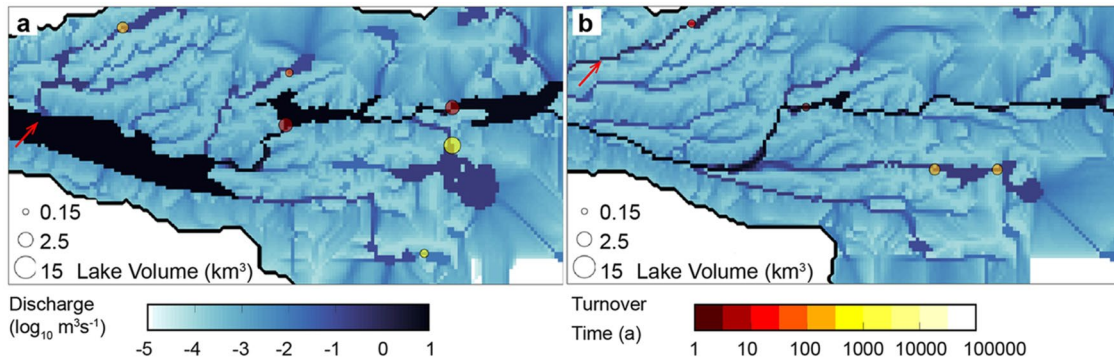
Figure 7. Subglacial water fluxes, lake volumes and turnover times for the inset area in Figures 5 and 6 for 14 ka BP. (a) $k = 0.8$; (b) $k = 1.0$. Key as in Figures 5 and 6.

and decrease upstream, as would be expected, but there is no apparent trend with k value (Figures S4c and S4d in Supporting Information S1). However, discharge is generally lower for 20 ka (average is 23% lower at 20 ka for $k = 0.8$ or 0.9; note this is only for discharges that decrease), reflecting the lower subglacial water production rates at this time (which must be due to lower strain rates because ice thicknesses were greater at 20 ka; Figure S1). Given the decrease in lake volume as k increases, lake turnover times also decrease with increasing k (Table 2). More generally, lake turnover is predicted to occur on timescales ranging from a few years to several hundreds of years. As an example, for the case $k = 0.9$ at 20 ka the minimum turnover time is 3 years, maximum is 900 years, and average turnover time is 156 years; the equivalent numbers at 14 ka are 3 years, 434 years, and 90 years, respectively.

4. Discussion

4.1. Processes of Bedrock Erosion in Marguerite Trough Channels

The morphology of the channels on the floor of Marguerite Trough, specifically their anastomosing and bifurcating patterns with undulating long profiles and abrupt terminations (Figures 1a, 1b,, and 3a), confirm that the channels were eroded by pressurized subglacial water flowing at high velocities (e.g., Kirkham et al., 2020; Lowe & Anderson, 2003; Nitsche et al., 2013; Shreve, 1972; Sugden et al., 1991). Recent systematic analyses of channel metrics and considerations of bedrock erosion rates performed by Kirkham et al. (2019, 2020) indicate that channels as large as those in Marguerite Trough most likely formed progressively through several glacial cycles on timescales of 10^5 years. The morphological observations we make here from the palaeo-ice stream bed in Marguerite Trough are consistent with these interpretations but also shed light on the processes acting to erode the ice-stream bed on spatial scales down to tens of meters.

The occurrence of potholes, from small (meter-scale) to giant scales (kilometer-scale), are clear evidence of rapidly flowing, turbulent water with enough potential energy to carry bedload to erode the hollows through abrasion and corrosion. The giant potholes we identify (Figures 3b–3d) are around the same order of magnitude as the largest potholes mapped in the meltwater-eroded landscapes of the Transantarctic Mountains (TAM) at the edge of the East Antarctic Ice Sheet, although the largest potholes there have diameters of up to 300 m (Sugden & Denton, 2004) and our largest pothole is around 1,200 m in diameter. For comparison, the largest potholes of the well-known Channeled Scabland landscape in Washington State, USA are only ~100 m across (e.g., Baker, 2009). The water-scoured landscapes in both the TAM and Washington State are associated with episodic releases of water although the former in a subglacial setting and the latter in a proglacial setting (Baker, 2009; Bretz, 1969; Lewis et al., 2006). The small potholes and depressions with meter-scale diameters (Figure 2g), which are more consistent in scale with the majority of potholes identified in the TAM (Denton & Sugden, 2005), and overdeepenings at the bases of some channel walls (Figures 2c and 2d) indicate preferential incision at the channel sides, at least in some locations. Thus, based on our unique high-resolution seafloor observations we suggest that incision at the sides of channel floors could be through pothole formation and linkage. However, the occurrence of an anastomosing network of small channels in the confluence between two channels (Figure 3a) shows that incision is not always focussed at the sides of the larger channels. In that setting, incision was spread across the confluence floor as a network of smaller channels, implying net deepening of the wider

depression or basin through channels a few hundreds of meters wide but only a few tens of meters deep. It is not clear from our data whether those channels formed via pothole incision followed by linking, or whether the smaller channels may have migrated across the confluence floor to deepen the entire area but we do not favor the latter in a hard bedrock setting. If small, linked potholes are present as the building blocks for the channels, post-incision sedimentation as observed from the ROV video footage and bottom photographs (Figure 2g) likely obscures these meter-scale features; we further note that such small features also cannot be resolved by shipborne systems in these water depths.

We also recognize some confluences that have a pothole-like appearance at their upstream ends suggesting that some confluences may have originally formed as large potholes (Figure S3a); this process has been suggested for the formation of other Antarctic channel confluence areas in the TAM (Figure S3b, Lewis et al., 2006; Sugden et al., 1991). We note that, as for Marguerite Trough, some potholes in The Labyrinth area of the TAM are not well connected to channels (Figure S3b), which is also the case for the largest potholes in Marguerite Trough. We do not know why some of the potholes in Marguerite Trough attained such large sizes but one possible explanation is that the features have formed over multiple glacial cycles as has been suggested for the channel systems (Graham et al., 2009; Kirkham et al., 2020). The argument that the bedrock type in Marguerite Trough might favor erosion of larger forms is not particularly convincing given the volcanic/plutonic rock types of the area (Larter et al., 1997), which are similar to the bedrock types that the Channeled Scablands (basalt) or Labyrinth (dolerite) channels are incised into; thus, we prefer an explanation that invokes a longer period of (repeated) incision for the giant potholes.

Another pronounced feature only revealed by the ROV bathymetry is the stepped profile of several channel side-walls, with steep to near-vertical steps occurring at the bottoms of one of the channels (Figures 2c and 2d). The steep gradients of the step walls (50°–80°) suggests that they have formed in bedrock (see Movie S2) with the occurrence of stepped profiles probably indicating multi-stage incision. Both Larter et al. (2019) and Kirkham et al. (2019) have recognised "composite" channel forms in other Antarctic bedrock channels, and they suggested that glacial ice had reoccupied meltwater-carved channels widening their upper cross sections through glacial erosion. If this was the case for the stepped channel we describe here, and the step represents the depth to which ice had relaxed into the channels, then this would indicate ice occupying the upper 86% of the channel area with the bottom 14% of the channel (equates to 55 m in the vertical) being eroded by meltwater. We accept that this suggestion is based on only one example and should be treated with caution, however, the high-resolution nature of the bathymetry allows us to constrain how much of the channel may have been filled with ice versus subglacial water. This remains a significant unknown in these channel systems (cf. Kirkham et al., 2019) although models suggests water depths of only a few meters are needed to allow for significant bedrock erosion via abrasion (Fagherazzi et al., 2021).

In summary, the identification of previously unresolvable potholes, small channels at the base of larger channels, and complex channel cross-profile geometries suggest that the bedrock channels experienced multi-stage incision through a number of processes. Channel inception may have resulted from the linkage of potholes created by fast-flowing subglacial meltwater. Over time, sustained incision at the base of the channels, possibly through networks of smaller channels, combined with the excavation of the upper channel cross section by glacial erosion, led to the progressive widening and deepening of the channels. These processes would have gradually generated larger features when repeated over multiple glacial periods (Graham et al., 2009; Kirkham et al., 2019, 2020; Nitsche et al., 2013).

4.2. Character of Subglacial Water Flow

Low subglacial water fluxes across Antarctica have led previous studies to conclude that continuous, steady-state water flow would be insufficient to incise meltwater channels of the scale observed both in deglaciated settings beyond the margins of the present ice sheet (Kirkham et al., 2019; Lowe & Anderson, 2003; Nitsche et al., 2013), as well as beneath the extant ice sheet (Jordan et al., 2010; Rose et al., 2014). The low steady-state water fluxes for the Marguerite Trough catchment (typically $<10 \text{ m}^3 \text{ s}^{-1}$) are no exception and are consistent with the idea that the huge bedrock channels there probably formed over a long period of time and multiple glacial cycles (cf. Kirkham et al., 2019).

The hydrological modeling results (Figures 5 and 6) indicate that subglacial water would have been available across the Marguerite Trough palaeo-ice stream bed during both full-glacial and deglaciation stages. There is a large subglacial catchment that drains linearly through George VI Sound and into the Marguerite Trough at 20 ka and at 14 ka (Figures 5a and 6a), and by inference therefore, throughout deglaciation. However, the complex subglacial topography of this region means that there are many locations in which subglacial lakes could form. Given that episodic drainage of subglacial lakes is quite common in the present day (Smith, Fricker, et al., 2009, for instance, documented 124 individual drainage events observed in IceSAT data over a 4.5 year period, between 2003 and 2008; Siegfried & Fricker, 2018, found a further 20 events from a total of 45 lakes from 2008 to 2018), it would seem likely that deglacial water flow in the Marguerite Trough region could have been characterized by numerous episodic lake outburst events of various magnitudes and periodicities. The question of whether modern Antarctic lake drainage events, which largely occur from shallow "ponds" in hydropotential lows (e.g., Fricker et al., 2007; Smith, Gourmelen, et al., 2017; Wingham et al., 2006), are comparable with drainage events from lakes within bedrock depressions has been somewhat answered by the modeling studies of Pattyn (2008). In that paper, modeled drainage was from subglacial lakes located in 400 m-deep circular bed depressions, far deeper than the shallow "ponds" described for modern Antarctic lakes. Furthermore, their model results are similar whether lake drainage was initiated by small changes in ice thickness (and therefore hydraulic gradients) or a small influxes of water into the cavity (Pattyn, 2008), which is akin to our input of water from upstream catchments. Thus, we continue with the thought experiment here.

Given the incomplete understanding of the mechanisms driving lake recharge and outbursts (e.g., Malczyk et al., 2020; Siegert et al., 2016), estimating the magnitude and frequency of outburst events for the Marguerite Trough area is difficult. However, if we use inferences from present-day observational and model-based studies we can begin to explore the possible characteristics of these events. In one of the first Antarctic lake drainage events to be documented, Wingham et al. (2006) observed a 1.8 km^3 drainage event in the Adventure subglacial trough in East Antarctica, which occurred over 18 months, yielding a mean discharge of ~50 m^3 s^{-1}. If we use this timeframe to scale the possible drainage of lakes in the Marguerite Trough area (and assume $k = 0.8$ for the moment), the largest lake (A; see Figure 5a for location) could yield discharges of ~1,000 m^3 s^{-1}, with a possible return period of 100–200 years. Higher in the catchment, lakes G and H could yield discharges of ~500 m^3 s^{-1} at periodicities of 1,000–2,000 years, which would presumably pass through the system, as they would effectively overwhelm the lower, smaller lakes along the drainage axis. The smaller lakes themselves could produce fluxes of 10–100 m^3 s^{-1}, at periodicities of less than 10 to around 100 years. Thus, the main drainage path would seem likely to experience a complex range of magnitudes and frequencies of drainage events, with frequent small outbursts punctuated by occasional, much larger events. Numerical modeling studies have demonstrated that even relatively small but frequent influxes of water to the subglacial environment (~10 m^3 s^{-1}) may have a significant erosive impact on bedrock channel excavation when repeated regularly over glacial timescales (Beaud et al., 2016, 2018). Thus, even relatively small releases of water from trapped subglacial lakes are likely to lead to an incremental growth in bedrock channel size when repeated over hundreds to thousands of years.

It is important to note that these are all mean discharges. In a modeling study of the Adventure subglacial trough region, using the data from Wingham et al. (2006), Peters et al. (2009) found that whilst subglacial discharge between the lakes in the study area was very sensitive to model parameters (and especially the assumed channel roughness), short-lived peak fluxes around 10 times the mean discharge were quite possible. This could allow short-lived outbursts of up to 10,000 m^3 s^{-1} in the Marguerite Trough region. Such events could cause rapid erosion of subglacial bedrock channels (cf. Kirkham et al., 2019). We would like to point out that even though the largest discharges we predict here (~10^3 m^3 s^{-1}) are about three times the reported values for contemporary subglacial lake drainages (e.g., Wingham et al., 2006), they are smaller than previous estimates for discharge from Antarctic subglacial lake drainages (~10^5 m^3 s^{-1}; Evatt et al., 2006; Kirkham et al., 2019) and they are also smaller than the observed peak discharges observed for Icelandic jökulhlaups (10^4 m^3 s^{-1}; Björnsson, 2002). As a result, we consider our results to be within a plausible range for subglacial discharge rates and the reader is referred to Kirkham et al. (2019) for further discussion.

The sensitivity of the calculated water flow paths to changing k values mirrors the sensitivity of inferred water flow paths reported in present-day hydrological reconstructions of Antarctica to small variations in the surface topography and, therefore, the assumed subglacial water pressure (Napoleoni et al., 2020; Smith, Gourmelen, et al., 2017; Wright et al., 2008). Recent work has, however, pointed out the importance of bed topography for

determining water flow paths and accumulation areas and that unrealistically smooth Antarctic bed elevation models (based on interpolation in no data areas) will bias lake locations and sizes (MacKie et al., 2020). With our offshore data set this problem is much less relevant as bathymetric DEMs have resolutions on the order of several tens of meters (compared to Antarctic-wide DEMs that have resolutions of several hundreds of meters at best); on the other hand, factors like ice thickness and surface slope for palaeo-ice sheet beds can only be obtained from model results and are thus uncertain, especially on short time-scales. Another factor may be related to the shape of the bed depressions because model results suggest that lake shape can significantly affect the stability of a subglacial lake, particularly if lakes are elongate in ice-flow directions (Pattyn, 2008), as we might expect in Marguerite Trough (e.g., Figures 1a, 5, and 6). Subglacial water pressures are likely to vary considerably over time, particularly if water discharge through the subglacial drainage system varies markedly. This would mean that some channels may become inactive (or carry much smaller water fluxes) over longer or shorter periods of time, and could therefore be plastered with subglacial till, whereas other areas may stay active or experience later increases in water flux, and then exhibit bare bedrock surfaces, matching observations of variable sediment infill within bedrock channels in other offshore regions (Nitsche et al., 2013; Smith, Hillenbrand, et al., 2009). This could explain the occurrence of typical glacial-deglacial-postglacial sediment sequences in these (Figure 4) and many West Antarctic marine channels, as well as the scarcity of sorted sediments (e.g., note the absence of outwash fans or depocentres in Figure 1b) that we might expect to be deposited from subglacial meltwater (e.g., Smith, Hillenbrand, et al., 2009). An alternative, or perhaps complementary suggestion, is that the channels are mainly active during ice-sheet advance as water trapped in upstream basins is squeezed out, and therefore more "typical" deglacial sedimentary sequences are deposited and preserved in the channels as the ice sheet recedes. Some support for this scenario may be derived from our modeling results, for example, if we consider that some lakes ave turnover times of 100–1000s of years (G and H; Table 2) then they may only drain a few times during deglaciation adding further weight to the conclusion that the channels form over multiple glacial cycles.

Against these ideas, however, is the result that calculated subglacial lake volumes are much smaller at higher k values (representing water at closer to ice overburden pressure; e.g., Table 2). This reduction is caused by the increasing dominance of ice thickness (and ice surface slope) on the subglacial hydraulic potential at higher water pressures. This effectively forces water through bedrock overdeepenings; as long as the adverse bed slope is less than ~11 times the ice surface slope (Shreve, 1972), water can effectively flow uphill, out of all but the largest or steepest overdeepenings in the bed topography. In this case, the drainage system seems more likely to experience much more constant, and much lower, water fluxes. Modeling the complex interactions between ice dynamics and basal hydrology, especially at the scale of an ice sheet, is still at an early stage, making it difficult to argue unequivocally for high or low basal water pressures. The variability of hydrological conditions at the ice-sheet bed on the shortest time-scales (weeks to years) is thought to have been captured by observations of modern lake drainage events with some lakes appearing to be continuously connected, others having only intermittent connections, and connectivity between lakes evolving and increasing over time (e.g., Malczyk et al., 2020; Smith, Gourmelen, et al., 2017).

Calculated subglacial melt rates in Marguerite Trough are relatively high; up to 40 mm a^{-1}, with a mean of 11.7 mm a^{-1} for 20 ka, and 11.9 mm a^{-1} for 14 ka, compared with other modeled ice sheet-wide means (e.g., 2.0 mm a^{-1} [Willis et al., 2016], 3.5 mm a^{-1} [Llubes et al., 2006], and 5.3 mm a^{-1} [Pattyn, 2010]). In general, higher water discharge beneath ice sheets is associated with lower water pressure, as the greater frictional heating due to the flowing water allows larger, more efficient tunnels to open, overcoming the ice overburden pressure (as has been observed in summer on the Greenland Ice Sheet, e.g., Banwell et al., 2016; Chandler et al., 2013). The high water availability in the Marguerite Trough area, which may be related to relatively high geothermal heat flux in the area (e.g., An et al., 2015; Martos et al., 2017), could therefore allow water pressures some way below the ice overburden pressure to occur, which in turn would allow larger subglacial lakes to form in the area (e.g., Table 2), potentially giving the much more varied basal water flux, with occasional, substantial outburst events discussed above.

4.3. Implications

Accepting uncertainties around subglacial water pressures, the hydrological modeling investigations undertaken for the Marguerite Trough palaeo-ice stream bed suggest a reasonable supply of subglacial meltwater is available, especially for the 14-ka ice sheet. Episodic releases of this meltwater, as subglacial lakes filled and drained,

would have been capable of significant erosion in the bedrock channel systems. Thus, even if the mechanisms proposed by Alley et al. (2006) and Jordan et al. (2010) for trapping or generating water in subglacial lakes did occur during the last glacial as the ice advanced over Marguerite Trough and was eventually released, episodic outburst flooding events probably continued throughout deglaciation, as did channel erosion. One potential avenue for future research is to perform subglacial hydrological modeling experiments for an advancing Antarctic Ice Sheet to explore how much water can be trapped beneath the ice sheet, and how and when it is likely to drain.

The effect of episodic outbursts on the ice dynamics of a major palaeo-ice stream as it deglaciated are difficult to predict owing to uncertainties around the nature of the hydrologic system and ice thickness changes over short and long timescales. Active subglacial lake drainages beneath the modern ice sheet. albeit with smaller discharges and a soft sedimentary substrate, appear to only temporarily affect ice-flow velocities for periods of weeks to months and, over the course of a few years, the effect on overall ice-flow speed is thought to be negligible (Joughin et al., 2016; Smith, Gourmelen, et al., 2017). Flow routing of outburst waters through the well-defined bedrock channel systems may have acted as an efficient semi-permanent drainage network during deglaciation thus drawing subglacial water away from other areas, effectively increasing basal traction and acting as a stabilizing mechanism (cf. Lelandais et al., 2018; Schroeder et al., 2013). However, there is no geological or geomorphological evidence for a stillstand of the ice stream grounding zone during deglaciation on the inner continental shelf in Marguerite Trough (Livingstone et al., 2013; Ó Cofaigh et al., 2005, 2014); in fact, retreat in this area at around 10 ka is interpreted to have been rapid. This suggests that external environmental forcing during rapid retreat was strong enough to overcome any stabilization afforded by an efficient drainage network in the trough. Furthermore, if subglacial lake drainage events were episodic and relatively short-lived then the effect on grounding-line stability during retreat may also have been short-lived. Thus, we reiterate that care needs to be taken when interpreting the geological record of past water releases and their influence on deglacial ice dynamics but we maintain that deglaciated terrains can provide different and complementary information to glaciological observations of present-day ice sheets, particularly of ice-sheet beds and over timescales longer than a few decades.

5. Conclusions

The combination of high-resolution marine observations and hydrological modeling in a well-known bedrock channel system in Marguerite Trough, Antarctic Peninsula, allows for an in depth study of incision processes with meltwater sourced by the episodic drainage of subglacial lakes further upstream. Processes include pothole formation and the erosion of smaller channels within larger ones supporting the notion that Antarctic bedrock channels have attained their large sizes through multiples stages of erosion, including during deglaciation, and probably over several glacial cycles (Kirkham et al., 2019). These observations would not have been possible without the use of a remotely operated vehicle to obtain high-resolution imagery and bathymetry from the seafloor.

Numerical modeling of water accumulation (as subglacial lakes) and routing beneath the Marguerite Trough palaeo ice stream suggests that basal water fluxes are likely to have been both spatially and temporally variable during deglaciation. We show that both accumulation (size of lakes) and flow pathways are sensitive to changes in water pressures, suggesting that the palaeo-ice stream bed experienced a range of hydrological conditions with some channels active at the same time as others were filled with ice. This, plus the episodic nature of subglacial water flow, may explain the relative scarcity of meltwater-related deposits in marine sediment cores.

Recharge rates for the subglacial lakes in bedrock are typically tens to hundreds of years, implying that multiple drainage events would have occurred during the deglacial phase of a glacial cycle. Even if subglacial lakes that may have formed during ice-sheet advances (Alley et al., 2006; Jordan et al., 2010), and subsequently drained, were responsible for the initial incision of the anastomosing channels, we conclude that there was enough water available at the ice-sheet bed to continue eroding the channels during the deglacial phase, albeit in multiple phases.

Conflict of Interest

The authors declare no conflicts of interest relevant to this study.

Data Availability Statement

Multibeam bathymetry echosounder data (MBES; acquired by ship systems) were reprocessed and gridded using the open-source software MB-System (https://www.mbari.org/products/research-software/mb-system/). MBES data acquired by UK research vessels (JR59, JR71, JR157) can be accessed by request stating the geographic area of interest or the cruise ID to the Polar Data Centre (https://www.bas.ac.uk/data/uk-pdc/) and the *Isis* ROV data can be accessed as a dataset directly (https://doi.org/10.5285/EF1996E4-7825-4456-B1F7-4D1B26531D72). See Dowdeswell et al. (2021) for further details; no registration is required. MBES data from US vessels (all NBP cruises) can be accessed through the Rolling Deck To Repository (www.rvdata.us) and selecting the "Search Cruises" and "Nathaniel B. Palmer"; no registration is required.

References

Alley, R. B., Dupont, T., Parizek, B., Anandakrishnan, S., Lawson, D. E., Larson, G., & Evenson, E. (2006). Outburst flooding and the initiation of ice-stream surges in response to climatic cooling: A hypothesis. *Geomorphology*, *75*(1–2), 76–89. https://doi.org/10.1016/j.geomorph.2004.01.011

An, M., Wiens, D. A., Zhao, Y., Feng, M., Nyblade, A., Kanao, M., et al. (2015). Temperature, lithosphere-asthenosphere boundary, and heat flux beneath the Antarctic Plate inferred from seismic velocities. *Journal of Geophysical Research: Solid Earth*, *120*(12), 8720–8742. https://doi.org/10.1002/2015jb011917

Anderson, J. B., & Oakes Fretwell, L. (2008). Geomorphology of the onset area of a paleo-ice stream, Marguerite Bay, Antarctic Peninsula. *Earth Surface Processes and Landforms*, *33*(4), 503–512. https://doi.org/10.1002/esp.1662

Arndt, J. E., Schenke, H. W., Jakobsson, M., Nitsche, F. O., Buys, G., Goleby, B., et al. (2013). The international bathymetric chart of the southern ocean (IBCSO) version 1.0: A new bathymetric compilation covering circum-Antarctic waters. *Geophysical Research Letters*, *40*(12), 3111–3117. https://doi.org/10.1002/grl.50413

Arnold, N. (2010). A new approach for dealing with depressions in digital elevation models when calculating flow accumulation values. *Progress in Physical Geography*, *34*(6), 781–809. https://doi.org/10.1177/0309133310384542

Baker, V. R. (2009). The channeled scabland: A retrospective. *Annual Review of Earth and Planetary Sciences*, *37*, 393–411. https://doi.org/10.1146/annurev.earth.061008.134726

Banwell, A., Hewitt, I., Willis, I., & Arnold, N. (2016). Moulin density controls drainage development beneath the Greenland ice sheet. *Journal of Geophysical Research: Earth Surface*, *121*(12), 2248–2269. https://doi.org/10.1002/2015jf003801

Beaud, F., Flowers, G. E., & Venditti, J. G. (2016). Efficacy of bedrock erosion by subglacial water flow. *Earth Surface Dynamics*, *4*(1), 125–145. https://doi.org/10.5194/esurf-4-125-2016

Beaud, F., Venditti, J. G., Flowers, G. E., & Koppes, M. (2018). Excavation of subglacial bedrock channels by seasonal meltwater flow. *Earth Surface Processes and Landforms*, *43*(9), 1960–1972. https://doi.org/10.1002/esp.4367

Bell, R. E. (2008). The role of subglacial water in ice-sheet mass balance. *Nature Geoscience*, *1*(5), 297–304. https://doi.org/10.1038/ngeo186

Bell, R. E., Studinger, M., Shuman, C. A., Fahnestock, M. A., & Joughin, I. (2007). Large subglacial lakes in East Antarctica at the onset of fast-flowing ice streams. *Nature Climate Change*, *445*(7130), 904–907. https://doi.org/10.1038/nature05554

Benn, D., & Evans, D. J. (2010). *Glaciers and glaciation*. Routledge.

Bentley, M. J., Johnson, J. S., Hodgson, D. A., Dunai, T., Freeman, S. P. H. T., & Cofaigh, C. Ó. (2011). Rapid deglaciation of Marguerite Bay, western Antarctic Peninsula in the early Holocene. *Quaternary Science Reviews*, *30*(23–24), 3338–3349. https://doi.org/10.1016/j.quascirev.2011.09.002

Bjarnadóttir, L. R., Winsborrow, M., & Andreassen, K. J. G. (2017). Large subglacial meltwater features in the central Barents Sea. *Geology*, *45*(2), 159–162.

Björnsson, H. (2002). Subglacial lakes and jökulhlaups in Iceland. *Global and Planetary Change*, *35*, 255–271.

Bretz, J. H. (1969). The Lake Missoula floods and the channeled scabland. *The Journal of Geology*, *77*(5), 505–543. https://doi.org/10.1086/627452

Chandler, D. M., Wadham, J. L., Lis, G. P., Cowton, T., Sole, A., Bartholomew, I., et al. (2013). Evolution of the subglacial drainage system beneath the Greenland Ice Sheet revealed by tracers. *Nature Geoscience*, *6*(3), 195–198. https://doi.org/10.1038/ngeo1737

Denton, G. H., & Sugden, D. E. (2005). Meltwater features that suggest Miocene ice-sheet overriding of the Transantarctic Mountains in Victoria Land, Antarctica. *Geografiska Annaler - Series A: Physical Geography*, *87*(1), 67–85. https://doi.org/10.1111/j.0435-3676.2005.00245.x

Domack, E., Amblas, D., Gilbert, R., Brachfeld, S., Camerlenghi, A., Rebesco, M., et al. (2006). Subglacial morphology and glacial evolution of the Palmer deep outlet system, Antarctic Peninsula. *Geomorphology*, *75*(1–2), 125–142. https://doi.org/10.1016/j.geomorph.2004.06.013

Domack, E. W., Jacobson, E. A., Shipp, S., & Anderson, J. B. (1999). Late Pleistocene–Holocene retreat of the West Antarctic ice-sheet system in the Ross Sea: Part 2—Sedimentologic and stratigraphic signature. *The Geological Society of America Bulletin*, *111*(10), 1517–1536. https://doi.org/10.1130/0016-7606(1999)111<1517:lphrot>2.3.co;2

Dowdeswell, J., Larter, R., Noormets, R., Griffiths, G., & Hogan, K. (2021). Isis remotely-operated vehicle (ROV) bathymetry data in Marguerite Trough, Antarctica, from James Clark Ross cruise JR157, 2007 (version 1.0) [Data set]. NERC EDS UK Polar Data Centre. https://doi.org/10.5285/EF1996E4-7825-4456-B1F7-4D1B26531D72

Dowdeswell, J. A., Noormets, R., Evans, J., Griffiths, G., Larter, R. D., & Ó Cofaigh, C. (2007). A comparison of swath-bathymetric imagery from high-latitude glacier-influenced fjords derived from AUV, ROV and shipboard systems. In K. Collins, & G. Griffiths (Eds.), *Collaborative autosub science in extreme environments* (pp. 47–54). NERC.

Dowdeswell, J. A., Ó Cofaigh, C., & Pudsey, C. (2004). Thickness and extent of the subglacial till layer beneath an Antarctic paleo–ice stream. *Geology*, *32*(1), 13–16. https://doi.org/10.1130/g19864.1

Evatt, G. W., Fowler, A. C., Clark, C. D., & Hulton, N. R. J. (2006). Subglacial floods beneath ice sheets. *Philosophical Transactions of the Royal Society A*, *364*, 1769–1794. https://doi.org/10.1098/rsta.2006.1798

Fagherazzi, S., Baticci, L., Brandon, C. M., & Rulli, M. C. (2021). Bedrock erosion in subglacial channels. *PLoS One*, *16*(9), e0253768. https://doi.org/10.1371/journal.pone.0253768

Flowers, G. E. (2015). Modelling water flow under glaciers and ice sheets. *Proceedings of the Royal Society A: Mathematical, Physical*, *471*(2176), 20140907. https://doi.org/10.1098/rspa.2014.0907

Fricker, H. A., Scambos, T., Bindschadler, R., & Padman, L. (2007). An active subglacial water system in West Antarctica mapped from space. *Science*, *315*(5818), 1544–1548. https://doi.org/10.1126/science.1136897

Glasser, N. F., & Sambrook Smith, G. H. (1999). Glacial meltwater erosion of the mid-Cheshire ridge: Implications for ice dynamics during the late Devensian glaciation of northwest England. *Journal of Quaternary Science*, *14*, 703–710. https://doi.org/10.1002/(sici)1099-1417(199912)14:7<703::aid-jqs465>3.0.co;2-9

Golledge, N. R., Fogwill, C. J., Mackintosh, A. N., & Buckley, K. M. (2012). Dynamics of the last glacial maximum Antarctic ice-sheet and its response to ocean forcing. *Proceedings of the National Academy of Sciences*, *109*(40), 16052–16056. https://doi.org/10.1073/pnas.1205385109

Golledge, N. R., Levy, R. H., McKay, R. M., Fogwill, C. J., White, D. A., Graham, A. G. C., et al. (2013). Glaciology and geological signature of the last glacial maximum Antarctic ice sheet. *Quaternary Science Reviews*, *78*, 225–247. https://doi.org/10.1016/j.quascirev.2013.08.011

Golledge, N. R., Menviel, L., Carter, L., Fogwill, C. J., England, M. H., Cortese, G., & Levy, R. H. (2014). Antarctic contribution to meltwater pulse 1A from reduced Southern Ocean overturning. *Nature Communications*, *5*(1), 1–10. https://doi.org/10.1038/ncomms6107

Graham, A. G., Larter, R. D., Gohl, K., Hillenbrand, C.-D., Smith, J. A., & Kuhn, G. (2009). Bedform signature of a West Antarctic palaeo-ice stream reveals a multi-temporal record of flow and substrate control. *Quaternary Science Reviews*, *28*(25–26), 2774–2793. https://doi.org/10.1016/j.quascirev.2009.07.003

Graham, A. G. C., Larter, R. D., Gohl, K., Dowdeswell, J. A., Hillenbrand, C.-D., Smith, J. A., et al. (2010). Flow and retreat of the late Quaternary pine Island-Thwaites palaeo-ice stream, West Antarctica. *Journal of Geophysical Research*, *115*, F03025. https://doi.org/10.1029/2009JF001482

Heroy, D. C., & Anderson, J. B. (2007). Radiocarbon constraints on Antarctic Peninsula ice sheet retreat following the last glacial maximum (LGM). *Quaternary Science Reviews*, *26*(25–28), 3286–3297. https://doi.org/10.1016/j.quascirev.2007.07.012

Hogan, K. A., Dowdeswell, J. A., Larter, R. D., Ó Cofaigh, C., & Bartholomew, I. (2016). Subglacial meltwater channels in Marguerite Trough, western Antarctic Peninsula. Geological Society London Memoirs, 46, 215–216. *In* J. A. Dowdeswell, et al. (Eds.), *Atlas of submarine glacial landforms: Modern, quaternary and ancient*. https://doi.org/10.1144/m46.178

Huvenne, V. A., Tyler, P. A., Masson, D. G., Fisher, E. H., Hauton, C., Huehnerbach, V., et al. (2011). A picture on the wall: Innovative mapping reveals cold-water coral refuge in submarine canyon. *PLoS One*, *6*(12), e28755. https://doi.org/10.1371/journal.pone.0028755

Jamieson, S. S., Ross, N., Greenbaum, J. S., Young, D. A., Aitken, A. R., Roberts, J. L., et al. (2016). An extensive subglacial lake and canyon system in Princess Elizabeth Land, East Antarctica. *Geology*, *44*(2), 87–90. https://doi.org/10.1130/g37220.1

Jordan, T., Ferraccioli, F., Corr, H., Graham, A., Armadillo, E., & Bozzo, E. (2010). Hypothesis for mega-outburst flooding from a palaeo-subglacial lake beneath the East Antarctic Ice Sheet. *Terra Nova*, *22*(4), 283–289.

Joughin, I., Shean, D. E., Smith, B. E., & Dutrieux, P. (2016). Grounding line variability and subglacial lake drainage on Pine Island Glacier, Antarctica. *Geophysical Research Letters*, *43*(17), 9093–9102. https://doi.org/10.1002/2016gl070259

Kamb, B., Raymond, C. F., Harrison, W. D., Engelhardt, H., Echelmeyer, K. A., Humphrey, N., et al. (1985). Glacier surge mechanism: 1982-1983 surge of variegated glacier, Alaska. *Science*, *227*(4686), 469–479. https://doi.org/10.1126/science.227.4686.469

Kehew, A. E., Piotrowski, J. A., & Jørgensen, F. (2012). Tunnel valleys: Concepts and controversies: A review. *Earth-Science Reviews*, *113*(1–2), 33–58. https://doi.org/10.1016/j.earscirev.2012.02.002

Kennedy, D. S., & Anderson, J. B. (1989). Glacial-marine sedimentation and quaternary glacial history of Marguerite Bay, Antarctic Peninsula. *Quaternary Research*, *31*(2), 255–276. https://doi.org/10.1016/0033-5894(89)90008-2

Kilfeather, A. A., Cofaigh, C. Ó., Lloyd, J. M., Dowdeswell, J. A., Xu, S., & Moreton, S. G. (2011). Ice-stream retreat and ice-shelf history in Marguerite Trough, Antarctic Peninsula: Sedimentological and foraminiferal signatures. *Bulletin*, *123*(5–6), 997–1015. https://doi.org/10.1130/b30282.1

Kirkham, J. D., Hogan, K. A., Larter, R. D., Arnold, N. S., Nitsche, F. O., Golledge, N. R., & Dowdeswell, J. A. (2019). Past water flow beneath pine Island and Thwaites glaciers, West Antarctica. *The Cryosphere*, *13*(7), 1959–1981. https://doi.org/10.5194/tc-13-1959-2019

Kirkham, J. D., Hogan, K. A., Larter, R. D., Arnold, N. S., Nitsche, F. O., Kuhn, G., et al. (2020). Morphometry of bedrock meltwater channels on Antarctic inner continental shelves: Implications for channel development and subglacial hydrology. *Geomorphology*, *370*, 107369. https://doi.org/10.1016/j.geomorph.2020.107369

Kuhn, G., Hillenbrand, C.-D., Kasten, S., Smith, J. A., Nitsche, F. O., Frederichs, T., et al. (2017). Evidence for a palaeo-subglacial lake on the Antarctic continental shelf. *Nature Communications*, *8*(1), 1–10. https://doi.org/10.1038/ncomms15591

Larter, R. D., Hogan, K. A., Hillenbrand, C.-D., Smith, J. A., Batchelor, C. L., Cartigny, M., et al. (2019). Subglacial hydrological control on flow of an Antarctic Peninsula palaeo-ice stream. *The Cryosphere*, *13*(6), 1583–1596. https://doi.org/10.5194/tc-13-1583-2019

Larter, R. D., Rebesco, M., Vanneste, L. E., Gamboa, L. A. P., & Barker, P. F. (1997). Cenozoic tectonic, sedimentary and glacial history of the continental shelf west of Graham Land, Antarctic Peninsula: Geology and seismic stratigraphy of the Antarctic margin, Part 2. *American Geophysical Union Antarctic Research Series*, *71*, 1–27.

Lelandais, T., Ravier, É., Pochat, S., Bourgeois, O., Clark, C., Mourgues, R., & Strzerzynski, P. (2018). Modelled subglacial floods and tunnel valleys control the life cycle of transitory ice streams. *The Cryosphere*, *12*(8), 2759–2772. https://doi.org/10.5194/tc-12-2759-2018

Lewington, E. L. M., Livingstone, S. J., Clark, C. D., Sole, A. J., & Storrar, R. D. (2020). A model for interaction between conduits and surrounding hydraulically connected distributed drainage based on geomorphological evidence from Keewatin, Canada. *The Cryosphere*, *14*(9), 2949–2976. https://doi.org/10.5194/tc-14-2949-2020

Lewis, A. R., Marchant, D. R., Kowalewski, D. E., Baldwin, S. L., & Webb, L. E. (2006). The age and origin of the Labyrinth, western Dry Valleys, Antarctica: Evidence for extensive middle Miocene subglacial floods and freshwater discharge to the Southern Ocean. *Geology*, *34*(7), 513–516. https://doi.org/10.1130/g22145.1

Livingstone, S., Cofaigh, C. Ó., Hogan, K., & Dowdeswell, J. (2016). Submarine glacial-landform distribution along an Antarctic Peninsula palaeo-ice stream: A shelf–slope transect through the Marguerite Trough system (66–70°S). *Geological Society London Memoirs*, *46*(1), 485–492. https://doi.org/10.1144/m46.180

Livingstone, S. J., Cofaigh, C. Ó., Stokes, C. R., Hillenbrand, C.-D., Vieli, A., & Jamieson, S. S. (2013). Glacial geomorphology of Marguerite Bay palaeo-ice stream, western Antarctic Peninsula. *Journal of Maps*, *9*(4), 558–572. https://doi.org/10.1080/17445647.2013.829411

Livingstone, S. J., Stokes, C. R., Ó Cofaigh, C., Hillenbrand, C.-D., Vieli, A., Jamieson, S. S., et al. (2016). Subglacial processes on an Antarctic ice stream bed. 1: Sediment transport and bedform genesis inferred from marine geophysical data. *Journal of Glaciology*, *62*(232), 270–284. https://doi.org/10.1017/jog.2016.18

Llubes, M., Lanseau, C., & Rémy, F. (2006). Relations between basal condition, subglacial hydrological networks and geothermal flux in Antarctica. *Earth and Planetary Science Letters*, *241*(3–4), 655–662. https://doi.org/10.1016/j.epsl.2005.10.040

Lowe, A. L., & Anderson, J. B. (2003). Evidence for abundant subglacial meltwater beneath the paleo-ice sheet in Pine Island Bay, Antarctica. *Journal of Glaciology*, *49*(164), 125–138. https://doi.org/10.3189/172756503781830971

MacKie, E. J., Schroeder, D. M., Caers, J., Siegfried, M. R., & Scheidt, C. (2020). Antarctic topographic realizations and geostatistical modeling used to map subglacial lakes. *Journal of Geophysical Research: Earth Surface*, *125*(3), e2019JF005420. https://doi.org/10.1029/2019jf005420

Malczyk, G., Gourmelen, N., Goldberg, D., Wuite, J., & Nagler, T. (2020). Repeat subglacial lake drainage and filling beneath Thwaites glacier. *Geophysical Research Letters*, *47*(23), e2020GL089658. https://doi.org/10.1029/2020gl089658

Martos, Y. M., Catalán, M., Jordan, T. A., Golynsky, A., Golynsky, D., Eagles, G., & Vaughan, D. G. (2017). Heat flux distribution of Antarctica unveiled. *Geophysical Research Letters*, *44*(2211), 11417–11426. https://doi.org/10.1002/2017gl075609

Napoleoni, F., Jamieson, S. S. R., Ross, N., Bentley, M. J., Rivera, A., Smith, A. M., et al. (2020). Subglacial lakes and hydrology across the Ellsworth subglacial highlands, West Antarctica. *The Cryosphere*, *14*, 4507–4524. https://doi.org/10.5194/tc-14-4507-2020

Nitsche, F. O., Gohl, K., Larter, R. D., Hillenbrand, C. D., Kuhn, G., Smith, J. A., et al. (2013). Paleo ice flow and subglacial meltwater dynamics in Pine Island Bay, West Antarctica. *The Cryosphere*, *7*(1), 249–262. https://doi.org/10.5194/tc-7-249-2013

Ó Cofaigh, C., Davies, B. J., Livingstone, S. J., Smith, J. A., Johnson, J. S., Hocking, E. P., et al. (2014). Reconstruction of ice-sheet changes in the Antarctic Peninsula since the last glacial maximum. *Quaternary Science Reviews*, *100*, 87–110.

Ó Cofaigh, C., Dowdeswell, J. A., Allen, C. S., Hiemstra, J. F., Pudsey, C. J., Evans, J., & Evans, D. J. A. (2005). Flow dynamics and till genesis associated with a marine-based Antarctic palaeo-ice stream. *Quaternary Science Reviews*, *124*(5–6), 709–740. https://doi.org/10.1016/j.quascirev.2004.10.006

Ó Cofaigh, C., Evans, J., Dowdeswell, J. A., & Larter, R. D. (2007). Till characteristics, genesis and transport beneath Antarctic paleo-ice streams. *Journal of Geophysical Research*, *112*, F03006. https://doi.org/10.1029/2006JF000606

Ó Cofaigh, C., Pudsey, C. J., Dowdeswell, J. A., & Morris, P. (2002). Evolution of subglacial bedforms along a paleo-ice stream, Antarctic Peninsula continental shelf. *Geophysical Research Letters*, *29*(8), 41–414144.

Pattyn, F. (2008). Investigating the stability of subglacial lakes with a full Stokes ice-sheet model. *Journal of Glaciology*, *54*(185), 353–361. https://doi.org/10.3189/002214308784886171

Pattyn, F. (2010). Antarctic subglacial conditions inferred from a hybrid ice sheet/ice stream model. *Earth and Planetary Science Letters*, *295*(3–4), 451–461. https://doi.org/10.1016/j.epsl.2010.04.025

Peters, N. J., Willis, I. C., & Arnold, N. S. (2009). Numerical analysis of rapid water transfer beneath Antarctica. *Journal of Glaciology*, *55*(192), 640–650. https://doi.org/10.3189/002214309789470923

Peterson, G., & Johnson, M. D. (2018). Hummock corridors in the south-central sector of the Fennoscandian ice sheet, morphometry and pattern. *Earth Surface Processes and Landforms*, *43*(4), 919–929. https://doi.org/10.1002/esp.4294

Prothro, L. O. N. (2018). *Glacial retreat patterns and processes on Antarctic continental margins*. Rice University. Retrieved from https://hdl.handle.net/1911/105911

Rignot, E., Fenty, I., Xu, Y., Cai, C., & Kemp, C. (2015). Undercutting of marine-terminating glaciers in West Greenland. *Geophysical Research Letters*, *42*(14), 5909–5917. https://doi.org/10.1002/2015gl064236

Rose, K. C., Ross, N., Bingham, R. G., Corr, H. F., Ferraccioli, F., Jordan, T. A., et al. (2014). A temperate former West Antarctic ice sheet suggested by an extensive zone of subglacial meltwater channels. *Geology*, *42*(11), 971–974. https://doi.org/10.1130/g35980.1

Sawagaki, T., & Hirakawa, K. (1997). Erosion of bedrock by subglacial meltwater, Soya Coast, East Antarctica. *Geografiska Annaler - Series A: Physical Geography*, *79*(4), 223–238. https://doi.org/10.1111/1468-0459.00019

Schroeder, D. M., Blankenship, D. D., & Young, D. A. (2013). Evidence for a water system transition beneath Thwaites glacier, west Antarctica. *Proceedings of the National Academy of Sciences*, *110*(30), 12225–12228. https://doi.org/10.1073/pnas.1302828110

Shaw, J., & Gilbert, R. J. G. (1990). Evidence for large-scale subglacial meltwater flood events in southern Ontario and northern New York State. *Geology*, *18*(12), 1169–1172. https://doi.org/10.1130/0091-7613(1990)018<1169:ef1ssm>2.3.co;2

Shreve, R. (1972). Movement of water in glaciers. *Journal of Glaciology*, *11*(62), 205–214. https://doi.org/10.1017/s002214300002219x

Siegert, M. J., Ross, N., & Le Brocq, A. M. (2016). Recent advances in understanding Antarctic subglacial lakes and hydrology. *Philosophical Transactions of the Royal Society A: Mathematical. Physical Engineering Sciences*, *374*, 20140306. https://doi.org/10.1098/rsta.2014.0306

Siegfried, M. R., & Fricker, H. A. (2018). Thirteen years of subglacial lake activity in Antarctica from multi-mission satellite altimetry. *Annals of Glaciology*, *59*, 76pt1, 42–55. https://doi.org/10.1017/aog.2017.36

Simkins, L. M., Anderson, J. B., Greenwood, S. L., Gonnermann, H. M., Prothro, L. O., Halberstadt, A. R. W., et al. (2017). Anatomy of a meltwater drainage system beneath the ancestral East Antarctic ice sheet. *Nature Geoscience*, *10*(9), 691–697. https://doi.org/10.1038/ngeo3012

Smith, B. E., Fricker, H. A., Joughin, I. R., & Tulaczyk, S. (2009). An inventory of active subglacial lakes in Antarctica detected by ICESat (2003–2008). *Journal of Glaciology*, *55*(192), 573–595. https://doi.org/10.3189/002214309789470879

Smith, B. E., Gourmelen, N., Huth, A., & Joughin, I. (2017). Connected subglacial lake drainage beneath Thwaites glacier, west Antarctica. *The Cryosphere*, *11*(1), 451–467. https://doi.org/10.5194/tc-11-451-2017

Smith, J. A., Andersen, T. J., Shortt, M., Gaffney, A. M., Truffer, M., Stanton, T. P., et al. (2017). Sub-ice-shelf sediments record history of twentieth-century retreat of Pine Island Glacier. *Nature*, *541*(7635), 77–80. https://doi.org/10.1038/nature20136

Smith, J. A., Graham, A. G., Post, A. L., Hillenbrand, C. D., Bart, P. J., & Powell, R. D. (2019). The marine geological imprint of Antarctic ice shelves. *Nature Communications*, *10*(1), 1–16. https://doi.org/10.1038/s41467-019-13496-5

Smith, J. A., Hillenbrand, C.-D., Larter, R. D., Graham, A. G., & Kuhn, G. (2009). The sediment infill of subglacial meltwater channels on the West Antarctic continental shelf. *Quaternary Research*, *71*(2), 190–200. https://doi.org/10.1016/j.yqres.2008.11.005

Stearns, L. A., Smith, B. E., & Hamilton, G. S. (2008). Increased flow speed on a large East Antarctic outlet glacier caused by subglacial floods. *Nature Geoscience*, *1*(12), 827–831. https://doi.org/10.1038/ngeo356

Storrar, R. D., Stokes, C. R., & Evans, D. J. (2014). Morphometry and pattern of a large sample (>20,000) of Canadian eskers and implications for subglacial drainage beneath ice sheets. *Quaternary Science Reviews*, *105*, 1–25. https://doi.org/10.1016/j.quascirev.2014.09.013

Sugden, D., & Denton, G. (2004). Cenozoic landscape evolution of the Convoy range to Mackay glacier area, Transantarctic Mountains: Onshore to offshore synthesis. The *Geological Society of America Bulletin*, *116*(7–8), 840–857. https://doi.org/10.1130/b25356.1

Sugden, D. E., Denton, G. H., & Marchant, D. R. (1991). Subglacial meltwater channel systems and ice sheet overriding, Asgard range, Antarctica. *Geografiska Annaler - Series A: Physical Geography*, *73*(2), 109–121. https://doi.org/10.1080/04353676.1991.11880335

Willis, I. C., Pope, E. L., Gwendolyn, J.-M., Arnold, N. S., & Long, S. (2016). Drainage networks, lakes and water fluxes beneath the Antarctic ice sheet. *Annals of Glaciology*, *57*(72), 96–108. https://doi.org/10.1017/aog.2016.15

Wingham, D. J., Siegert, M. J., Shepherd, A., & Muir, A. S. (2006). Rapid discharge connects Antarctic subglacial lakes. *Nature Climate Change*, *440*(7087), 1033–1036. https://doi.org/10.1038/nature04660

Wright, A. P., Siegert, M. J., Le Brocq, A. M., & Gore, D. B. (2008). High sensitivity of subglacial hydrological pathways in Antarctica to small ice sheet changes. *Geophysical Research Letters*, *35*(17). https://doi.org/10.1029/2008gl034937